1984

Electronic Structure of Small Iron Clusters.

Keeyung Lee
Louisiana State University and Agricultural & Mechanical College

INFORMATION TO USERS

This reproduction was made from a copy of a document sent to us for microfilming. While the most advanced technology has been used to photograph and reproduce this document, the quality of the reproduction is heavily dependent upon the quality of the material submitted.

The following explanation of techniques is provided to help clarify markings or notations which may appear on this reproduction.

1. The sign or "target" for pages apparently lacking from the document photographed is "Missing Page(s)". If it was possible to obtain the missing page(s) or section, they are spliced into the film along with adjacent pages. This may have necessitated cutting through an image and duplicating adjacent pages to assure complete continuity.

2. When an image on the film is obliterated with a round black mark, it is an indication of either blurred copy because of movement during exposure, duplicate copy, or copyrighted materials that should not have been filmed. For blurred pages, a good image of the page can be found in the adjacent frame. If copyrighted materials were deleted, a target note will appear listing the pages in the adjacent frame.

3. When a map, drawing or chart, etc., is part of the material being photographed, a definite method of "sectioning" the material has been followed. It is customary to begin filming at the upper left hand corner of a large sheet and to continue from left to right in equal sections with small overlaps. If necessary, sectioning is continued again—beginning below the first row and continuing on until complete.

4. For illustrations that cannot be satisfactorily reproduced by xerographic means, photographic prints can be purchased at additional cost and inserted into your xerographic copy. These prints are available upon request from the Dissertations Customer Services Department.

5. Some pages in any document may have indistinct print. In all cases the best available copy has been filmed.

University
Microfilms
International

300 N. Zeeb Road
Ann Arbor, MI 48106

ELECTRONIC STRUCTURE OF SMALL IRON CLUSTERS

A Dissertation

Submitted to the Graduate Faculty of the
Louisiana State University and
Argicultural and Mechanical College
in partial fulfillment of the requirements
for the degree of
Doctor of Philosophy

in

The Department of Physics and Astronomy

by
Keeyung Lee
B.S., Seoul National University, Seoul, Korea, 1972,
M.S., Sogang University, Seoul, Korea, 1975
May 1984

TO MY MOTHER

AND

MY WIFE

ACKNOWLEDGMENTS

The author wishes to express his deep gratitude to Professor J. Callaway for guidance and supervision throughout this research.

Many thanks are also due to the Physics Department and all its members for the good will and help throughout his graduate study period. Especially, the author wishes to thank S. Dhar who provided essential help in some part of this work and A. Ziegler and K. Kwong for their help in the later period of this work.

Helpful discussions with Professor A. J. Freeman and D. E. Ellis of Northwestern University and D. D. Koelling of Argonne National Laboratory and many others in both institutions are gratefully appreciated.

Final thanks go to LSU SNCC for providing excellent technical services in computer use and to J. Grant for fast and flawless typing of this dissertation.

The author acknowledges support by the LSU Physics Department in the form of Teaching Assistantship from 1977 to 1982 and in the form of Research Assistantship from 1982 to 1984 provided through a grant to Dr. J. Callaway by the U. S. Army Research Office under Contract No. DAAG29-K-81-0006

TABLE OF CONTENTS

LIST OF TABLES

LIST OF FIGURES

ABSTRACT

The linear combination of Gaussian orbitals (LCGO) method has been adopted in developing a spin-polarized molecular orbital calculation code. The calculations are based on density functional theory using local density approximation for the exchange-correlation potential. A variational fitting method is used to obtain a charge density fit to avoid the need for using four-center integrals in evaluating the Coulomb potential. The matrix elements of the exchange potential are evaluated by direct numerical integration using a doubling grid developed for this purpose. Self-consistent solutions have been obtained using this method for Fe_9 and Fe_{15} clusters with open boundaries and with body-centered cubic symmetries. The convergence of several properties to those of bulk has been examined, and a good similarity could be obtained between the bulk density of states and that of Fe_{15} confirming the result obtained from the multiple-scattering (MS)-Xα method. The charge and spin densities for the central atom were found to be very different from those of bulk iron in agreement with the results reported by other authors. However, present results seem to exhibit stronger tendency of minority-spin electron flow to the central site than was obtained by MS-Xα method. The ionization potential of the Fe_9 cluster is determined by the transition state method and good agreement with experiment is obtained. Fe_8C and $Fe_{14}C$ clusters have also been considered to study impurity effects in clusters.

CHAPTER I

INTRODUCTION

There has been increasing interest during recent years in the local atomic environment in a solid due to the beliefs shared by many groups of physicists that many properties of solids are almost determined by interactions in the local atomic environment.[1,2] This concept has some experimental support and regards boundary conditions as having relatively little influence on the overall electronic structure.[3-5]

This topic has been extensively reviewed and is formulated as the Invariance Theorem (though it is not a rigorous theorem) which states that the density of states and especially the integrated density of states is relatively an invariant quantity independent of boundary conditions.[2]

There are other topics which motivate current interest in the local atomic situation. These include surface science, amorphous materials and crystalline solids with impurities or with aperiodic symmetry such as alloys. This work is a contribution to those aspects of physics where the model of perfect lattice periodicity is not appropriate.

Though the existence of situations with an essential lack of periodicity is the main motive for interest in the local electronic picture, application of this point of view will also be helpful in describing a system with perfect crystalline symmetry, but with emphasis given to local situations such as bonding interactions. By abandoning

the Bloch representation, we can have a better physical picutre of local interactions between an atom and its nearest neighbors in which the situation is viewed using chemical bonding concepts.

In such a description, almost all information is expected to be contained in the local density of states

$$n(E,\vec{r}) = n(E)|\psi_E(\vec{r})|^2$$

where $n(E)$ is the total density of states of the system. The idea that the local density of states has an 'invariance property' regardless of boundary conditions has a long history starting from Friedel's pioneering work in connection the theory of dilute random alloys.[2] But theoretical confirmations of such a view could not be attempted until recently due to difficulties in computation as will be discussed later. Recently there have been disputes about this point by several authors and lack of more convincing results confirming this point of view still leaves some doubts on this idea.[6,7]

Although the idea of considering an atom in its local environment with arbitrary boundary conditions to represent an atom in an extended periodic lattice could be a different problem than that raised by the above argument, there has been an attempt to identify the central atom plus some neighbors in an open boundary condition as equivalent to the atom in a bulk environment.[8] Such an attempt could have been stimulated by experimental evidences such as follows.[3] The ferromagnetic ordered alloy Fe_3Al has a body-centered cubic symmetry having two types of iron

sites: The D-site for which all eight neighbors are also iron atoms, and the A-site where only four of its neighbors are iron atoms. What is remarkable about this example is that the magnetic moment measured on D-site is 2.14 Bohr magnetons (μ_B), close to that for an atom in bulk iron 2.2 μ_B (the magnetic moment on A-site is 1.46). In this example, just one shell of iron neighborations was enough to make a D-site iron atom have the moment characteristic of pure bulk material. We should note however, that this example does not have open boundary conditions. With an open boundary condition and limited number of neighbors the central atom may behave very differently from a solid atom. In fact, a theorem by von Laue[9] suggests that the local density of states of the central site for a free cluster cannot become similar to that of a bulk site unless the central site is located far from the boundary, which means a very large cluster. Part of our objective is to study the properties of local atoms for different types of boundary conditions.

We have discussed an example for which the local environment mainly determines the physical properties of the central atom. As examples which can support the notion of 'invariance property', many amorphous materials showing significant amounts of crystalline properties can also be considered.[10] It is believed that these amorphous materials nevertheless have significant amounts of short range order which are responsible for crystalline properties (however, there has been some controversy on this point recently). If the 'invariance property' could find some basis, then cluster calculations could be a good starting point for discussing situations such as liquids or glasses.

There are quite a lot of problems for which cluster calculations could be useful. Consider systems containing impurities, hydrogen impurities in transition metal systems, for example. The remarkable phenomenon that the density of hydrogen per unit volume is greater in some metal hydrides than in either liquid or solid hydrogen makes such a system a very fascinating one.[13] Carbon impurities in iron provides another example. It is well-known that the mechanical properties of iron depend strongly on its carbon impurity content. This system has been of enormous practical interest in human history but no significant theoretical study on this system has been done so far.[14]

Other than such atomic impurities or vacancy problems, magnetic impurities (such as iron, nickel, etc.) in non-magnetic hosts such as copper are other types of situations where a cluster approach can be effective. We could hope to have some explanations on phenomena such as the Kondo effect from first principles calculations.[8] The Kondo effect could be explained so far only by many-body theory using an s-d interaction model.

Other than impurity problems, surface structure calculations could be another area of application.[15] There has been a tremendous amount of interest on surface problems in recent years. Though a cluster system cannot be directly related to a solid surface system, it certainly can give a good physical picture of surface structure for finite size clusters at least. Small transition metal clusters are known to be very important in catalysis. It is also known that catalytic properties of small transition metal clusters less than 10Å in size are quite dif-

ferent from those of solid surfaces.[16] Through calculations of such clusters, we may have some explanations on why the transition metals play such an important role in catalysis, through surface structure analysis. Transition metals also seem to play an important role in certain biological systems such as enzymes and proteins.[17] Iron in hemoglobin is an example. These systems may be too complex to be handled by present techniques, but it could be possible to understand such systems through cluster calculations in the future.

There has been enormous progress in molecular orbital calculations in recent years due to interest in the areas mentioned and to the development of high speed computers. Unlike solids or atoms, molecular systems usually require a very large orbital basis. In solids with periodicity, Bloch's theorem reduces the size of the orbital basis to that required for a single unit cell. But in molecular orbital calculations, some types of approximations are always made due to the necessity of a large orbital basis. Sometimes these approximations are quite severe.

The most successful methods dealing with large clusters include the multiple-scattering (MS)-$X\alpha$ method and the Discrete Variational Method (DVM).[18,19] The MS-$X\alpha$ method is a cluster version of the Green's function method (or KKR method) used in band structure calculations and employs muffin-tin approximation to the crystal potential in an essential way. A variety of systems have been studied using this method and it has proved itself to be a reliable method which can produce reasonable results. Attempts to prove the 'invariance property' from

sophisticated first-principles calculations was made for the first time using this method with reasonable success. But lack of more convincing results following this work using other methods led to objections to the conclusions made from the results of this method, especially by those who used the Hartree-Fock method.[7] Other results from a local density approximation calculation using a different method should help settle this dispute.

The DVM is another powerful method which depends completely on numerical integration technique.[20,21] In this method, every integral needed for the calculation is determined by direct numerical integration using a grid based on the Diophantine method.[22] Complete dependence on numerical integration is DVM's advantage as well as its disadvantage. For example, this method can employ any type of orbital basis and can handle systems with arbitrary geometry, whereas the MS-Xα method is not suitable for systems like diatomic molecules. On the other hand, this method adopts a fitting of the charge density and has to adopt frozen core approximation almost necessarily for transition metal systems to control the number of grid points used for integration. This method has been used extensively on many systems containing impurities and with embedding boundary conditions.[23,24]

Though it has never been used on large molecular systems, there is another method called LCAO-Xα which has been very successful for small molecular systems.[25,26] In this method, the charge density as well as the exchange-correlation potential is fitted by a sum of analytic functions. Results obtained using this method for diatomic molecular

systems have been given endorsement from a recent local density calculation in which almost no approximations were made at all.[27]

Other than the methods based on local density approximations which we have discussed, the Hartree-Fock (H-F) method may be worth mentioning though it has never been successfully used for transition metal systems. The H-F method has a well-known problem of generating zero density of states at the Fermi level in metals. Furthermore, due to the number of four-center integrals which increases as the fourth power of the size of the orbital basis, the H-F method cannot be used for large molecular systems without significant reduction in the size of the orbital basis.[28] Semi-empirical H-F methods which make drastic approximations for some integrals have been found to be very ineffective for transition metal systems.[29]

We have adopted a variational fitting method which will be described in detail in the next chapter, to avoid the troublesome four-center integrals needed for evaluating the Coulomb potential. The exchange-correlation potential has been treated exactly using a direct numerical integration approach. A doubling grid in three-dimensional space has been developed for this purpose.

Our method has been applied to Fe_9 and Fe_{15} cluster systems with open boundary conditions. Emphasis was given to checking the 'invariance property' of the density of states for these clusters. Also, properties of the central atom in these clusters were studied to check the feasibility of impurity containing cluster calculations. Our method has been developed for systems with full cubic point group

symmetry only. For systems with other types of symmetry, a new symmetrized orbital basis set needs to be found and a new set of grid points should be determined. In its present form, our method can be used for spin-polarized calculations in many other types of clusters having full cubic symmetry.

We can think of other problems which could be handled with the present method with proper embedding techniques. Once we have a suitable embedding condition with which the central atom in a cluster can be made similar to an atom in a bulk environment, we can replace that central atom with an impurity atom of our interest. This type of calculation could give us valuable informations about the properties of solids containing impurities.

In addition, we can consider spin impurity systems in connection with the transition state scheme. With an artificial constraint of keeping the central atom with no spin polarization (geometrical shapes such as Wigner-Seitz cell could be used for this purpose as a first approximation), we can determine the energy needed for flipping one spin in a system.[18] This energy obtained from a first principles calculation can be used to estimate the Curie temperature of ferromagnetic materials.

Another problem of interest is the Kondo effect. Considering that many-body approaches interpreted the situation only through the interaction of impurity d-electrons and host s-electrons, we could probably present a better explanation from first principles calculations in which there are not only d-s interaction but also d-p and d-d interactions.[69]

It is generally known that there are also significant overlap between d-electrons on different sites.

This dissertation is organized as follows: In Chapter II, the general outline of the method of calculation is discussed. This includes the general description of the computational techniques, review of the existing methods for molecular orbital calculations and a description of the method we used in the present work. In Chapter III, we will discuss the results obtained using the present method and a comparison with the results obtained from other methods will be made. Finally, the general conclusions we could make from the present work will be presented in Chapter IV. Appendix A discusses the grid points we used for numerical integration in this work. The symmetrized basis forms for the simple cubic, body-centered cubic, and face-centered cubic symmetry's first nearest-neighbor atomic arrangement are presented in Appendicies B, C, and D.

CHAPTER II

THE METHOD OF CALCULATION

This chapter consists of six sections. In Section A, a general description of computational techniques is presented. Section B contains a discussion of the tight-binding method which is the computational basis of present work. A review of the existing methods is presented in Section C and Sections D and E contains detailed description of the techniques we used for the Coulomb and the exchange potential matrix element evaluation. Finally, the actual computational procedure we followed to reach a self-consistent solution is described in Section F.

A. General Description

The question of how to describe the complicated potential for an electron moving in the field of other electrons is one of the most challenging topic in ab initio calculations. The true Hamiltonian we have to deal with is the many-body Hamiltonian

$$H = \sum_{i=1}^{N} \left[-\nabla_i^2 - \sum_{\ell} \frac{2 \cdot Z_\ell}{|\vec{r}_i - \vec{R}_\ell|} + \sum_{i,j=1}^{N}{}' \frac{1}{|\vec{r}_i - \vec{r}_j|}\right] + \sum_{\ell,\ell'}{}' \frac{Z_\ell Z_{\ell'}}{R_{\ell\ell'}}$$

in which the primes denote no summation for identical terms. (Rydberg unit of energy will be used throughout this dissertation.)

Attempts to solve this Hamiltonian by use of the variational principle led to the Hartree and Hartree-Fock one electron equations.[27] The traditional Hartree-Fock (H-F) method, which is still used extensively among chemists, has been disastrous in applications to solids.[54] For example, it generates zero density of states at the Fermi energy for metals and also gives very wide bandwidths to sp-bonded materials. The use of configuration interaction to incorporate electron correlations is successful in small systems but quite impractical for large ones. The major difficulty in application of the H-F method is the enormous number of four-center integrals to be evaluated which increases essentially as $(NB)^4$, where NB is the number of orbital basis being used.[28,31]

Due to such enormous difficulty encountered in obtaining exact H-F solutions, several semi-empirical approximations to this method such as

the Extended HUckel (E-H) and the complete neglect of differential overlap (CNDO) method appeared.[31] These approximations made the H-F equation somewhat easier to solve and were partly successful in describing simple systems with efficiency. But the semi-empirical molecular orbital calculations of transition elements are complicated by strong interactions of nearly free electron (NFE) like sp-orbitals and rather localized d-orbitals. This interaction causes hybridization of orbitals which is manifested clearly in the band structures of transition elements. In such a situation, it becomes quite difficult to estimate any semi-empirical parameters. A detailed comparison of the E-H and SCF-Xα-SW method when applied to transition metal clusters showed grave discrepancies in the results obtained, indicating the difficulties involved in proper parametrization in the semi-empirical methods.[16] The energy level distribution in the E-H method was very different from that of SCF-Xα-SW method, and a comparison with the bulk density of states showed no resemblance at all for the E-H result though the SCF-Xα-SW result gave a reasonable resemblance. It is interesting to note that whenever such large discrepancies occurred between cluster and solid properties due to too many approximations, these have usually been routinely attributed to the small cluster size, namely surface effect.

Although it has been pointed out that the semi-empirical methods within the H-F approximation are not effective, especially for the transition elements, and although these methods are becoming more obsolete in the present high-speed computer age, we give a brief review of this approach before going on to discussions on methods other than the

H-F method.

The importance of the E-H method lies in the fact that it is one of the pioneering methods which was simple enough to handle complex molecules. It was introduced in simplified form by Hückel[32] in 1931 and was further extended for better accuracy by others.[33,34] The principle idea in this method lies in approximating the diagonal elements of the Fock matrix by appropriate parameters such as ionization potentials and assuming the off-diagonal elements to be proportional to the overlap matrix elements such that

$$H_{\alpha\alpha} = -I_{\alpha}$$

$$H_{\alpha\beta} = 0.5\ K(H_{\alpha\alpha} + H_{\beta\beta})\ S_{\alpha\beta}$$

in which K is a parameter usually in the range 1.0-2.0. The CNDO is a more advanced form of approximating the H-F equations which assumes the overlap matrix to be diagonal. This method makes less severe approximations to Fock matrix elements than the E-H method but still carries a severe approximation providing no significant improvement in general over the E-H result.

We have discussed major difficulties in the H-F method and its poor behavior when applied to the transition elements. On the other hand, the local density approximation to the density functional theory of the exchange-correlation potential was found to produce remarkably good results in almost all problems with less computational difficulty. This

approach has started from the work of Slater[35] in which he sought to approximate the H-F equation which is easier to handle and practicable in more complicated systems. He rewrote the one electron H-F equation in a form

$$[-\nabla^2 + V_N + V_H + V_{xc}]\,\psi_n = E_n\psi_n$$

in which $V_N = -\sum_{\ell} 2Z_\ell/|\vec{r}-\vec{R}_\ell|$ is the nuclear attraction potential and

$$V_H = 2\int \frac{\rho(\vec{r}')}{|\vec{r}-\vec{r}'|}\, d^3\vec{r}'$$

is the Coulomb interaction potential between the electrons. V_{xc} is the non-local exchange potential written in a local potential form. It was suggested that $V_{xc} \sim [\rho(\vec{r})]^{1/3}$ can be used as an approximation to the actual non-local exchange potential. This result which was obtained as an approximation to the H-F equation later found its theoretical basis in the density functional theory which reproduced the same functional form with a slightly different factor using the free electron gas model.[36,37] There have been further improvements in the local density functional form afterwards and it has become indispensible in the ab initio calculations of solid state physics.[38,39] Obviously the great advantage of such a form results from the local nature of the exchange-correlation potential and a possibility of doing without four-center integrals.

Though it has become possible to have the one-electron Schrödinger equation with a local exchange-correlation potential, the numerical nature of its functional form again causes other types of computational difficulties. Due to the difficulties even in this simpler form in ab initio calculations, some sort of approximations are usually made in practice. These include the pseudo-potential approximation,[40] frozen core approximation,[20] and the semi-empirical methods within the local density approximation. The semi-empirical methods usually draw some information from an experiment or a very accurate computational result and put this in a parameterized form. Several attempts have been made to parametrize one electron calculation, employing fitting and interpolation, sometimes together with the pseudo-potential method.[41] These efforts certainly helped generate reasonable results with efficiency but the physical implications involved in the parameterization step could not always be made clear.

The frozen core approximation is another way of simplifying the complexities in real calculations and has been used extensively in the completely numerical discrete-variational method (DVM) in cluster calculations.[24] This approach exploits the well-known property that the core electrons are not influenced very much by bonding interactions, and assumes the core states to be the same as the atomic core states. A possible complication in this approximation is the problem of orthogonalizing the valence orbital basis to the core electron states for every atom in the cluster.[29]

Pseudo-potential approximation has been enormously successful in semiconductor calculations and could be another attractive approach. But so far it has not been exploited much in cluster calculations.[42] The handling of the angular momentum dependent (non-local) pseudopotential can be a possible difficulty in this case. The task of generating a reasonable pseudo-potential form for the transition metal atoms could be another problem, since singificant spatial overlap of the very localized d-electrons with the core orbitals could cause difficulty in properly incorporating the exchange-correlation potential contribution from the core electrons in the pseudo-potential.[43,44] This is due to the non-linear nature of local density functional form for charge density, i.e.,

$$(\rho_1 + \rho_2)^{1/3} \neq \rho_1^{1/3} + \rho_2^{1/3} \ .$$

In our present procedure, we have not employed any of the above approximations and have made straightforward calculations within the local density approximation. The only significant approximation we adopted is the charge density fitting which is done to make this procedure more practicable by avoiding the evaluation of too many four-center two-electron integrals which are needed if we want exact treatment of the Coulomb potential.

B. Tight Binding Method and Orbital Basis

Tight Binding method was proposed as far back as 50 years ago by F. Bloch,[45] but it has only been recently that any substantial amount of work based on this method have been accomplished.[46] This was mainly due to the difficulties in evaluating three-center integrals.[47] Therefore, this method was used mostly for qualitative description incorporating the semi-empirical approaches such as parameterization and fitting.[41]

This method has been given particular attention in recent years because it is particularly suitable for describing the local electronic structure which must be understood when dealing with systems without lattice periodicity. This method is also expected to be more appropriate for materials with less overlap of valence orbitals between neighboring atoms such as transition metals where we are primarily interested in the relatively localized d-electrons. A localized orbital basis approach has been enormously successful in the 3d-transition metal elements band structure calculations using the Gaussian type orbitals[46] and is also expected to be more effective than any other method in studying the local electronic structure of transition metal clusters.

In this method, a conceptual picture of the situation is very simple. A wave-function is expressed in terms of an appropriate set of orbitals such as Slater type orbitals (STO) or Gaussian type orbitals (GTO)[48] such that

$$\phi_{\alpha,\ell} = \phi_{\alpha}(\vec{r} - \vec{R}_{\ell})$$

$$\psi = \sum_{\alpha,\ell} a_\alpha \phi_{\alpha\ell} \quad .$$

In this case, α denotes the type of orbital at the site $\vec{R}_\ell$ on which it is centered. When ϕ_α's are the atomic orbitals itself, the method is called the Linear Combination of Atomic Orbitals (LCAO) method. Usually ϕ_α is not strictly an atomic orbital and could be either an independent Gaussian or a contracted combination of Gaussians in practical use.[28]

Gaussian type orbitals are usually preferred in molecular orbital calculations relative to STO's because of their advantage in evaluating the multi-center integrals. The multi-center integrals can be evaluated analytically in GTO basis set whereas straightforward analytic evaluations is not possible with STO's. The STO basis set is more appropriate in atomic calculations than in molecular orbital calculations and we have adopted GTO's as the basis function type in this procedure.

The main drawback of Gaussian type functions is that it does not resemble nicely the actual atomic orbitals in lacking cusp near the origin and in having an undesirable form far away from the origin.[31] The necessity of a large number of basis functions due to such unrealistic form is the main disadvantage in using this type of function. (Twice as many basis functions are generally needed for this type of function compared to the more realistic STO's.) The contraction of the basis set which restricts the relative freedom of the several independent Gaussians is usually adopted if the large number of basis functions causes difficulty.

The angular functions attached to each Gaussian type function are to be appropriately chosen depending upon the system of interest. In systems with a cubic group symmetry, the Kubic Harmonic functions are the natural choice and adopted in this work also as has been done in the band structure calculations of cubic metals,[46] namely (x,y,z)-type for the p-type orbital basis and x^2-y^2, $3z^2-r^2$, xy-, yz-, zx-type for the d-type orbital basis. For systems with symmetry other than cubic symmetry group, other types of angular functions could be considered. The angular function type should be chosen according to the principle of being able to describe the bonding and anti-bonding states properly.

Although the traditional Tight-Binding method has been used in a form of LCAO-method which takes the atomic orbitals as its basis set, we adopted independent Gaussian type orbitals in this work following the previous band calculations.[46] This choice is expected to give more flexibility for the core orbitals to readjust in the new environment which is important in molecular systems. But this also could cause excessive amounts of computer time.

With the given ansatz

$$\psi = \sum C_i \phi_i$$

the Schrödinger equation can be expressed as

$$H_{ij} C_j = E_i S_{ij} C_j$$

in which

$$H_{ij} \equiv \langle \phi_i | H | \phi_j \rangle$$

and

$$S_{ij} \equiv \langle \phi_i | \phi_j \rangle \ .$$

This leads to the Secular equation

$$| H_{ij} - E S_{ij} | = 0$$

for non-trival solutions of $\{C_i\}$. This condition gives the desired eigenvalues and eigenfunctions of the Hamiltonian matrix. In general, orbital basis ϕ_s's are not expected to be mutually orthogonal though they can be assumed to be normalized. Thus, the overlap matrix S is usually not a diagonal matrix. H_{ij} contains one-, two-, and three-center integrals and the terms can have the significance of on-site energies, hopping integrals, etc.[49]

The size of the matrix dimension for H and S equals the total number of orbital basis functions chosen for the system and it could become intolerably large for molecular systems. In systems with lattice periodicity, Bloch's theorem allows simplification to a much smaller size in matrix dimension determined by the number of functions needed to describe atoms in a single unit cell. For large molecular systems, it is almost inevitable to block-diagonalize the Hamiltonian matrix using the symmetry of a system whenever possible. This helps reduce the size

of matrix to be diagonalized and can be a critical factor for efficient calculation.

In this work, basis orbitals were put in symmetrized forms before starting the calculation for such purpose. The usual method of generating symmetrized basis is the projection operator technique.[50] Brief explanations of the generating procedure and tables of symmetrized basis forms generated for the simple cubic (SC), body-centered cubic (BCC) and face-centered cubic (FCC) nearest neighbor geometry are listed in the Appendix. For systems having a symmetry other than the full cubic group O_h, the same technique can be used to generate proper symmetrized basis sets.

Using the symmetrized form of the basis set can provide more computational advantages than just block diagonalizing the total Hamiltonian matrix. Consider the typical Hamiltonian matrix element

$$H_{ij}^{k\ell} \equiv < \chi_i^k \; |H| \; \chi_j^\ell >$$

in which χ_i^k denotes a symmetrized function belonging to k-th row of the i-th representation. It can be shown that

$$H_{ij}^{k\ell} = \frac{1}{d(i)} \delta_{ij} \delta_{k\ell} \sum_n H_{ii}^{nn}$$

if H is unchanged under all operations of the group such that $[P_\alpha, H] = 0$ for all operation $P\alpha$ in the group.[51] The Hamiltonian of a system is certainly invariant under any group operations. The above equation

shows that the matrix element H_{ii}^{kk} is independent of the row k, and all elements between the functions belonging to different representations i and j or different rows k and ℓ in the same representation are identically zero. This means that if the total Hamiltonian matrix is block-diagonalized, then many of the small blocks are identical (degenerate) if they belong to the same representation, i.e., in most cases we need to deal with only a single row in a given representation if it is degenerate.

Added to the above stated advantages, we have found the following property in the matrix element evaluation. For,

$$\chi_\mu = \sum_\ell a_\ell \phi_\ell$$

$$\chi_\nu = \sum_m a'_m \phi'_m$$

in which ϕ's are the independent Gaussians and a's are the coefficients in the symmetrized function, it was also found that

$$< a'_m \phi'_m \; | \chi_\mu > = |a'_m|^2 \cdot S_o$$

where

$$S_o \equiv < \phi'_1 | \chi_\mu > = < \phi'_2 | \chi_\mu > = \ldots.$$

Therefore, we have

$$< \chi_\mu | \chi_\nu > = \sum_m |a'_m|^2 \; < \phi'_1 | \chi_\mu >$$

allowing us to find the integral related to a single term in χ_ν if there are several terms in the combination. Furthermore, if the angular functions were given in a polynomial form such as $(x+y+z)\phi_\ell$, it was found in many cases that it is necessary to evaluate integrals related to just one term of the polynomial. Information was given in the input data as to whether such symmetry property could be used. This property was used in evaluating not only the overlap matrix but also the Hamiltonian matrix elements. All the information about the symmetrized orbital basis was provided as input data for the programs.

Choosing an appropriate set of exponents for the Gaussian functions is another important task in such variational calculations. The present work employed the same Gaussian exponents was used by Wachters in atomic self-consistent calculation,[52] which gives 14 s-type, 9 p-type and, 5 d-type orbitals to describe 3 d transition metal atoms. There are indications that orbital exponents of the atoms are not necessarily most appropriate for molecules as can be seen in the hydrogen molecule variational calculation. Though slight variations of the exponents can be expected to give better variational solution, it is not easy at all to determine which set of exponents is best suited for each different systems. Normal practice is to take the atomic orbital exponents unless other obvious modification is necessary.

C. Review of the Existing Methods

Before going into description of the procedure used in the present work in the following sections, several successful methods of cluster calculation being widely used will be discussed in this section. This will be helpful in understanding the difficulties involved in molecular orbital calculations and discussing relative merits between several different methods.

As has been discussed before, use of localized orbitals is undisputably natural and proper in describing local electronic structure in contrast to other types of bases such as plane waves. The Discrete Variational Method (DVM), LCAO-Xα, and Recursion Method are examples developed under this principle of tight-binding method. There has been another quite successful method called the Multiple Scattering-Xα (MS-Xα) developed as a cluster version of the KKR Green's function method in solid.[18] This method assumes muffin-tin potential approximation and can determine exact solution of the Schrödinger equation by numerical integration method within this potential approximation.

The DVM may be the most widely used method in the cluster calculations within the LCAO method. This method has been extensively used for large transition metal clusters as well as for small molecular systems.[20,53] This method has its basic characteristics in its completely numerical treatment of the calculation. Due to this property it can take any form of basis functions, sometimes even numerical basis. Because of its complete dependence on effectiveness of numerical

integration, DVM mostly resorts to frozen core approximation to control the number of points needed in the integration, for which the Diophantine integration scheme is usually adopted.[22] Due to the difficulty in evaluating the Coulomb potential at each grid point, charge density fitting is almost indispensible in this method such that

$$\tilde{\rho}(\vec{r}) = \sum_i a_i f_i(\vec{r}) \quad ,$$

where the $f(\vec{r})$ are a set of functions chosen for this purpose). Once such a form is obtained

$$V_c(\vec{r}_k) = \int \frac{\tilde{\rho}(\vec{r})}{|\vec{r} - \vec{r}_k|} \, d^3r$$

can be used to find the Coulomb potential at the necessary points and

$$(V_c + V_{xc})_{ij} = \sum_k W_k \, \chi_i(\vec{r}_k) \, \chi_j(\vec{r}_k) \cdot (V_c(\vec{r}_k) + V_{xc}(\vec{r}_k)$$

can be evaluated in a straightforward way. The main advantage of DVM lies in the freedom in choosing any form of basis and the ability to handle systems with arbitrary geometries. The main disadvantage of DVM lies in the limitation of the number of points it can take for numerical integration. This difficulty usually forces DVM to use frozen core approximation to limit the number of points in practical range. Use of the DVM has been quite successful in many impurity containing clusters and possible embedding conditions have also been explored.[24,53]

Another successful method in molecular calculations within the tight-binding approximation is the LCAO-Xα method, although this method has never been applied to large molecular systems. This method is essentially an extension of the work of Sambe et al.[25] in which the charge density and exchange-correlation potential were fitted into some analytic functions. By such extensive use of fitting, the necessity of four-center integrals for the Coulomb potential could be eliminated and the difficulty of handling numerical data for exchange-correlation potential could be avoided. Fitting of key quantities by use of simple analytic functions naturally provided good efficiency but the difficulty involved in the fitting remains to be the major obstacle in this method. The original least square fitting scheme for charge density was modified into the variational fitting scheme (see next section) for better fitting quality by Dunlap et al.[26] Bond-centered functions were also added to nuclear-centered fitting basis functions in their diatomic molecular calculation.[27] Their result with such elaborate fitting effort was proved to be quite satisfactory from the later work of Painter et al. in which exact treatment of the Coulomb potential using the four-center integrals was done.[55] Other than the cumbersome problem of choosing a proper fitting basis set, this method can give quite satisfactory results with efficiency. In our present work, we have adopted the variational fitting scheme used in this LCAO-Xα method.

Somewhat alien to the above described approaches, but another popular LCAO method for cluster calculations is the Recursion Method.[70] This ingenious approach for solving the Schrödinger equation from local

electronic point of view could be applied to clusters of even more than 100 atoms and to surface problems. However, realistic potentials can not be employed in this method. The main objective of the Recursion method in practical applications is limited to finding the local density of states of a system from localized orbital model. The main idea of this method is transformation of the Schrödinger equation into a chain model which should be determined appropriately for each particular system such that

$$H\ |U_n\rangle = a_n\ |U_n\rangle + b_{n+1}\ |U_{n+1}\rangle + b_n\ |U_{n-1}\rangle$$

The state $|U_n\rangle$, which is a linear combinatin of the localized orbital basis, is expected to represent the n-th shell from the central atom. The parameters a_n describe the coupling of each environment to itself and b_n the coupling to its neighbors.

We have described several successful approaches within the tight-binding method. These methods utilize the localized orbital basis to describe the local electronic structure. Completely different from the above types of approaches, but which has nevertheless been successful in many aspects is the MS-Xα method.[18] Major defect of this method is the artificial partitioning of space into muffin-tin type potentials. To handle the open boundary situation which does not occur in solids, a large sphere enclosing the whole cluster (called the Watson's sphere) is added to the otherwise normal muffin-tin potentials. Another muffin-tin type potential (spherically symmetric) is assumed in the region outside

this Watson's sphere. The shortcomings of this method are manifested most severely in systems like diatomic molecules, but otherwise this method could produce quite reasonable results with efficiency in many situations. A lot of our results obtained from the present calculation will be compared later with the results obtained from this Ms-Xα method.

We have described several successful methods in the molecular orbital calculations. The method we have used in this work for large transition metal clusters is not completely novel and could be regarded as a modification of some of the described methods. Specifically, we have adopted the variational fitting method for charge density as in the LCAO-Xα method. Our procedure for handling the exchange-correlation potential may be regarded as having the same technical implication as in DVM, the only difference being the different choice of grid points for its numerical integration.

D. Coulomb Potential and Charge Density Fitting

In this section, details of the charge density fitting are discussed in connection with the Coulomb potential matrix element evaluation. As has been pointed out, exact treatment of the Coulomb potential necessitates evaluation of the numerous time consuming four-center integrals in the tight-binding method.[28] This has been the major bottleneck in the H-F-Roothaan method (or LCAO-HF) and has been the main reason why the H-F method could not be applied to large molecular systems.

Though the four-center integrals (which are also called two-electron integrals among chemists) are an indispensible part of the H-F-Roothaan method in which both the Coulomb and exchange potential matrix elements are expressed in terms of these integrals, it is not the case in the local density approximation (LDA) method. Within the LDA scheme, the exchange-correlation potential has to be treated numerically and we are less dependent on the four-center integrals than in the H-F-Roothaan method. In fact, an appropriate approximation for treating the Coulomb potential is inevitable if the LDA method is to be practicable for large molecular systems. Use of the four-center integrals for exact Coulomb potential treatment without any approximation is also plausible in the LDA approach for small molecular systems but will face the same serious problem as in the H-F-Roothaan method as the system becomes large and, therefore, a large number of bases needed. One of the approximations being widely used at the moment is the charge density fitting. In this

approach, the charge density of a system is cast into some given form of analytic functions. This has the effect of reducing the number of integrals to be evaluated from being proportional to $(NB)^4$ to approximately $(NB)^3$, where NB is the number of orbital basis used.

Charge density fitting was first used by Sambe et al., in their small molecular system studies.[25] In their work the charge density was fit in a least-square sense, i.e., by minimizing the square of deviation in the fitted and real charge density. Dunlap et al. further modified this least square fitting method into the variational fitting method and used it in their diatomic molecular calculations.[27,56] Their idea was to minimize the error involved in the Coulomb energy due to fitting and not the charge density as in the least square fitting. Procedure for the multi-center charge density fitting is as follows: In the least square fitting method, the quantity to be minimized is defined as

$$D = \int d^3r \, [\rho(\vec{r}) - \tilde{\rho}(\vec{r})]^2$$

in which

$$\tilde{\rho}(\vec{r}) = \sum_{i=1}^{NFB} a_i f_i(\vec{r})$$

and $\{a_i\}$, $\{f_i(\vec{r})\}$ being the fitted coefficients and fitting bases respectively. NFB is the number of fitting bases employed. Although the fitted charge density is almost normalized, strict normalization can be achieved by demanding

$$\frac{\partial}{\partial a_i} [D + \lambda N] = 0 \quad (i=1, NFB)$$

in which

$$N = \sum_i \int a_i f_i(\vec{r})\, d^3r = \int \tilde{\rho}\, d^3r = \vec{a} \cdot \vec{n}$$

and

$$n_i = \int f_i(r)\, d^3r \ .$$

N is the total number of electrons in the system and λ the Lagrange multipler. Imposing the conditions

$$0 = \frac{\partial}{\partial a_i} [D + \lambda N] \quad , \quad (i=1, NFB)$$

we find the solution for $\vec{a}$ as

$$\vec{a} = S^{-1} (\vec{t} + \lambda \vec{n})$$

in which

$$S_{ij} = \int d^3r\, f_i(\vec{r})\, f_j(\vec{r})$$

$$t_i = \int d^3r\, \rho(\vec{r})\, f_i(\vec{r}) \quad .$$

Be requiring the normalization condition

$$N = \vec{n} \cdot \vec{a} = \vec{n} \cdot (S + \vec{t}) + \lambda \vec{n} \cdot (S^{-1} \vec{n})$$

we get

$$\lambda = \frac{N - \vec{n} \cdot (S^{-1} \vec{t})}{\vec{n} \cdot (S^{-1} \vec{n})}$$

for the Lagrange multiplier.

The variational fitting exactly follows this procedure except that the quantity to be minimized is replaced by

$$D' = \iint d^3r d^3r' \frac{(\rho(\vec{r}) - \tilde{\rho}(\vec{r}))\ (\rho(\vec{r}') - \tilde{\rho}(\vec{r}'))}{|\vec{r} - \vec{r}'|}$$

$$\equiv [\rho - \tilde{\rho} \mid \rho - \tilde{\rho}]$$

This means minimizing the error in the Coulomb energy due to fitting rather than the error in charge density. Definition of $\vec{t}$ and S should be replaced by

$$t'_j = [\rho(\vec{r}) \mid f_j(\vec{r}')]$$

$$S'_{ij} = [f_i(\vec{r}) \mid f_j(\vec{r}')]$$

where brackets are for expressions as is given in D'. These integrals

are special types of two-electron (four-center) integrals we discussed already. One of the great advantages we have in the Variational Fitting method is that the approximate value of total Coulomb energy of the system could be evaluated immediately out of the quantities already calculated. It can be shown easily that

$$U_C = [\rho(\vec{r}) \mid \rho(\vec{r}')]$$

$$= 2[\rho \mid \tilde{\rho}] - [\tilde{\rho} \mid \tilde{\rho}] + [\Delta\rho \mid \Delta\rho] \quad .$$

Therefore

$$U_C \tilde{=} 2 \sum_i a_i t'_i - \sum_i \sum_j a_i a_j S'_{ij}$$

in which the contribution from $[\Delta\rho \mid \Delta\rho]$ term has been neglected.

Superiority of the variational charge density fitting compared to other types of fitting schemes such as the least square fitting of charge density or potential has been discussed in detail by Mintmire et al.[56] There are several points worth mentioning about the computational advantages in the Variational Fitting (VF) relative to the least square fitting. First, three center integrals in $\vec{t}$ need not be calculated in the VF-Method. Evaluation of $\vec{t}'$ in the VF is necessary for the matrix element calculation anyway if we ask for the analytical evaluation of matrix element from the fitted charge density. Avoiding the evaluation of three-center integrals in $\vec{t}$ was found to give great savings in effort

and complexity as well as in computer time. Second, the VF can give quantities which can be a good check for the accuracy of fitting without any further effort. The quantities

$$[\rho \mid \tilde{\rho}] = \sum_i a_i \, t'_i$$

and

$$[\tilde{\rho} \mid \tilde{\rho}] = \sum_i \sum_j a_i \, a_j \, S'_{ij}$$

should be very close to each other for an acceptable fitting quality.

We could adopt the VF-method in this work because our choice of the Gaussian type orbital basis allows analytical evaluation of the two-electron integrals needed in the VF-method quite efficiently. It should be noted that the two-electron integrals cannot be evaluated by numerical means in practical sense due to its double space integral nature. The ability to evaluate two-electron integrals analytically also gives our method no restriction in performing all-electron calculation. The main reason why DVM has to adopt the frozen core approximation is due to the necessity of allocating very large number of points near the atomic centers around which the charge density is varying extremely rapidly. This is a very undesirable situation because atomic core region is the region of least interest due to its almost frozen characteristics. Therefore it is almost inevitable to have the frozen core approximation and least square fitting if the integral quantities needed in the fitting procedure are to be evaluated numerically.

The detailed steps for calculating the necessary quantities in fitting is as follows. Let

$$M_{ij}^{k} = \iint d^3r d^3r' \frac{f_k(\vec{r}') \chi_i(\vec{r}) \chi_j(\vec{r})}{|\vec{r} - \vec{r}'|}$$

$$\equiv [f_k \mid \chi_i \chi_j]$$

in which $\{f_k\}$ are the charge density fitting basis and $\{\chi_i\}$ are the symmetrized orbital basis. It can be noted that

$$M_{ij}^{k} = M_{ji}^{k}$$

and that M_{ij}^{k} is equivalent for symmetrized basis pairs (χ_i', χ_j') for all rows in a given representation. This is due to the fact that $\{f_k\}$ are the functions invariant under all group operations making up the specific point group and the selection rules property described in Chapter II, Section B. (It should be noted that $\{f_k\}$ are chosen to assume the same form as some of the symmetrized basis functions belonging to the identity representation, which are invariant under all point group operations.)

Consider the charge density expression belonging to some arbitrary representation R having dimension d(R)

$$\rho_R(\vec{r}) = \sum_{r=1}^{d(R)} \sum_{n=1}^{nocc} g_n \, |\psi_n^{(r)}|^2$$

in which r denotes rows and g_n the occupancy of the n-th energy level. Then the component of t_k' due to the representation R becomes

$$[t_k']_R = \iint d^3r d^3r' \frac{f_k(\vec{r}') \rho(\vec{r})}{|\vec{r} - \vec{r}'|}$$

$$= \sum_r \sum_r g_n \sum_i \sum_j C_{ni} C_{nj} [f_k \mid \chi_i^{(r)} \chi_j^{(r)}]$$

$$= \sum_r \sum_n g_n \sum_i \sum_j C_{ni} C_{nj} M_{ij}^k$$

in which M_{ij}^k has been used as a quantity independent of rows as has been discussed and $\{C_{ni}\}$ are the eigenfunction coefficients of the n-th energy level. It is assumed here that $\{C_{ni}\}$ have been made identical for different rows in a given representation by a proper normalization of the basis functions, making $\{C_{ni}\}$ independent of the rows.

Now we can discuss an important result out of this form. Because $\{g_n\}$, $\{C_{ni}\}$, and M_{ij}^k have been shown to be the quantities independent of different rows, we can put t_k' as

$$[t_k']_R = d(R) \left[\sum_n g_n \sum_{i,j} C_{ni} M_{ij}^k\right]$$

i.e., it is needed to evaluate this quantity only for any single row in a given representation R and simply multiply it by its degeneracy d(R).

In the actual calculation, this form was rearranged as

$$[t_k']_R = d(R) \cdot \sum_n g_n \left(2 \sum_{i=1}^{NB} \sum_{j=1}^{i} C_{ni} C_{nj} M_{ij}^k - \sum_{i=1}^{NB} C_{ni} C_{ni} M_{ii}^k\right)$$

exploiting the symmetry property of the matrix M. These steps can be reformulated for the spin polarized case in a straightforward way. Evaluation of other quantities needed for the variational fitting is trivial and will not be discussed.

Once the expression for the fitted charge density is obtained, such that

$$\tilde{\rho}(\vec{r}) = \sum_{k=1}^{NFB} a_k f_k(\vec{r})$$

then the matrix element can be found directly as follows.

$$\langle \chi_i | V_c(\vec{r}) | \chi_j \rangle = \sum_k a_k [f_k | \chi_i \chi_j]$$

$$= \sum_k a_k M_{ij}^k$$

we can see that the two-electron integral expressions $\{M_{ij}^k\}$ are the only major quantity needed for the entire process of fitting and matrix element evaluation. The VF-method is expected to give better accuracy for the total energy of a system than the LSF-method due to the very fact that it is based on the principle of minimization of the Coulomb energy error rather than the charge density error.

Though we have discussed the advantages which could be obtained from the fitting approach, there are also some difficulties in fitting itself. It has been reported that the fitting bases can become very unstable as the number of fitting bases is increased. Fitting method

using the exponential function type basis is a well-known ill-conditioned problem. The main difficulty comes from the fact that fitting basis functions are not linearly independent to each other for such functions. There is another difficulty in determining optimal basis set for the fitting, due to non-linear fitting problems. Fitting functions of different functional forms such as $e^{-\alpha r^2}$, $r^2e^{-\alpha r^2}$, etc. can be used to reduce the problem of linear dependency to each other but some undesirable situations could certainly occur as the size of fitting basis becomes very large.

Charge density fitting basis form was deduced from the symmetrized basis form belonging to the $\Gamma 1$-representation in cubic point group Oh. We used s-type symmetrized form as our fitting basis form for the simple- and r^2-type Gaussian fitting functions, i.e., $e^{-\alpha r^2}$ and $r^2e^{-\alpha r^2}$ respectively. It is obvious that r^2-type Gaussians have the same symmetry properties as that of the simple Gaussians. Exponents for the simple Gaussians were chosen to be double the s-type orbital exponents and the r^2-type Gaussian exponents were chosen to be double the p-type orbital exponents. This makes 23 fitting bases for each shell, giving a total of 46 fitting bases for the Fe_9 system and 69 fitting bases for the Fe_{15} system.

We have found that the r^2-type Gaussians improve fitting quality a lot, especially near the atomic core region around which the level structure is expectd to be rich. We also tried (x+y+z)-type fitting bases (with the same form as the p-type symmetrized basis) as an attempt to pursue improved fitting quality for Fe_9 system. Surprisingly, we

couldn't get any improvement in fitting quality. The fitted coefficients for such bases showed a systematic oscillatory behavior (from positive to negative signs for example) indicating its useless nature. However, such ℓ=1 type fitting basis with parabolic radial functional form (instead of the Gaussian) was reported to be effective for least square charge density fitting in the DVM calculation.[21]

We can also include ℓ=2 type fitting functions such as (xy,yz,zx)-type Gaussians or off-center Gaussian functions (such as bond-centered Gaussians used by Dunlap et al.[27]) as an attempt for better fitting quality. These type of functions have not been used in the present calculation.

E. Exchange-Correlation Potential

The very nature of local density functional type potential requires the exchange-correlation potential to be treated only by numerical means. Although this is the case, general trend for dealing with this potential has been to fit this into some analytical form for convenience. Although fitting itself needs numerical integration, analytical form obtained from the fitting can lead to simple and explicit evaluation of the matrix elements. On the other hand, attempt to handle such numerical function without an aid of fitting can be quite time consuming in the computer CPU time. We have considered both approaches in our work and have chosen the direct numerical evaluation approach rather that the fitting method. We describe the fitting procedure we tried in our work first and will discuss the doubling grid scheme we used for numerical integration next.

Fitting of the exchange-correlation (XC-) potential looks like an easier task than the fitting of charge-density because the XC-potential is a very slowly varying function in space. It certainly is not difficult but we have experienced some difficulty in obtaining a very good fit using the Gaussian type functions as fitting bases. For the multi-center XC-potential fitting purpose, bond-centered Gaussians could be of great help. But it should be noted that even in the fitting approach, use of very good grid points are indispensible in handling the numerical integrations needed for fitting.

Instead of following the conventional fitting procedure of using Gaussian type functions as the fitting bases, we have tried using the Kubic Harmonic functions $K_{\ell,1}(\theta,\phi)$'s which are the basis functions of different angular order for $\Gamma 1$-representation in Oh group.[57] There is a well-known theorem that the crystal field in systems having a cubic symmetry can be expanded in terms of these functions. One advantage of this idea is that once a good Kubic Harmonic fitting could be obtained, matrix elements can be evaluated exactly. Another advantage is the inclusion of correction to the Coulomb potential due to insufficient fitting accuracy using the Gaussian fitting basis only. It is a very attractive point that we can get corrections to the incomplete charge density fitting without much more effort.

We have not pursued this approach due to two main reasons. First difficulty was in the fitting itself. Though the Kubic Harmonic functions are very powerful bases of expansion, rapid variation of the necessary quantities near the ligand atomic centers caused great difficulty in getting a satisfactory fitting. For transition metal ligand atoms which have very localized d-orbitals near the atomic nucleus (peak probability position of d-electrons is located at around 0.5 a.u. from the nucleus), Kubic Harmonic functions of order as high as ℓ=10 was needed for an acceptable fitting at the first shell region with possibly higher order terms needed at the second shell region. Even with 28 special directions,[58] it was not easy to achieve satisfactory angular integrations in such situations. We concluded that this approach is not suitable for systems involving d-orbital electrons

though it could be acceptable for other systems such as aluminum clusters for which valence electrons are of delocalized character. Second difficulty was the ever increasing CPU time needed for the matrix element calculation as higher order Kubic Harmonic functions were included.

We adopted the direct numerical integration approach because the Kubic Harmonic fitting approach was not as efficient as we expected. For our numerical integration purpose, a doubling grid scheme in the three dimensional space of 1/48-th wedge zone was developed. For systems having full cubic point group Oh, which has 48 possible operations in its group, it can be shown that there are 48 equivalent space regions.

Though it is known that only a 1/48-th wedge zone is needed to be considered for such systems, another property from the group theory is essential in exploiting this property. Consider

$$(V^{XC})_{ij} = \int d^3r \; \chi_i^{(r)}(\vec{r}) \; V^{XC}(\vec{r}) \; \chi_j^{(r)}(\vec{r})$$

which is the matrix element between the symmetrized bases $\chi_i^{(r)}$ and $\chi_j^{(r)}$, which belong to the r-th row in a given representation. Though $V^{XC}(\vec{r})$ has been found to be invariant under all group operations,

$$\chi_i^{(r)}(\vec{r}) \cdot \chi_j^{(r)}(\vec{r})$$

product is not invariant in general, namely if $\chi_i^{(r)}(\vec{r})$ belongs to a degenerate representation. There is an important theorem in group theory related to this problem which is called the generalized Unsöld Theorem.[59] This theorem prescribes a method of generating an invariant function out of the basis of an irreducible representation. It says

$$\sum_{r=1}^{d(R)} |\chi^{(r)}|^2$$

is invariant under all operations of the group, in which d(R) is the degeneracy of the irreducible representation R. This is a generalization of the theorem by Unsöld which says that

$$\sum_{m=-\ell}^{\ell} | Y_{\ell m}(\theta,\phi)|^2$$

is invariant, in which $Y_{\ell m}$ are the spherical harmonics. Proof of the generalized Unsöld theorem is as follows.

Let P_α denote the rotation operator and $\Gamma(\alpha)_{ij}$ be the (i,j)-th element of matrix representation for operation α defined such that

$$P_\alpha \chi^{(j)} = \sum_{i=1}^{d(R)} \chi^{(i)} \Gamma(\alpha)_{ij}$$

Then,

$$P_\alpha \sum_{r=1}^{d(R)} |\chi^{(r)}|^2 = P_\alpha \sum_r \chi^{(r)*} \chi^{(r)}$$

$$= \sum_r \sum_{ij} \chi^{(i)*} \Gamma^*(\alpha)_{ir} \chi^{(j)} \Gamma(\alpha)_{jr}$$

$$= \sum_{ij} \chi^{(i)*} \chi^{(j)} \sum_r \Gamma(\alpha)_{jr} \Gamma(\alpha^{-1})_{ri}$$

$$= \sum_{ij} \chi^{(i)*} \chi^{(j)} \cdot \delta_{ji}$$

$$= \sum_{i=1}^{d(R)} |\chi^{(i)}|^2$$

in which unitary property of the representation has been used. The index for denoting the irreducible representation R has been suppressed in the above for simplicty. This important property of the symmetrized basis is essential in making direct numerical integration feasible by allowing us to deal with a 1/48-th zone of the space only.

During the process of doubling, we encountered a problem which makes the 'strict' doubling procedure quite unattractive. It demanded too many grid points to be generated if strict doubling was imposed. This problem could be resolved easily by taking approximately doubled length at one stage of the doubling process. About 1,300 points were generated for 9-atom (BCC) cluster system by having two sub-divisions in each division and 11 basic divisions. The details of doubling grid scheme is presented in Appendix A.

In the actual calculation of the matrix elements, we have not calculated some element and assumed it to be zero if the value of the

overlap integral related to that element were smaller than a certain number such as 10^{-6}. Because of the slowly varying characteristic of the XC-potential in space, this is expected to be a reasonable approximation. To make the iteration cycle more efficient, all the values of the basis product with the weight factor at each grid point multiplied, i.e.,

$$\chi_i(r_k)\ \chi_j(r_k)\ W_k$$

were calculated at a preparatory stage and stored. Furthermore, if this value was smaller than the number 10^{-8} at certain point k, it was taken to be zero and that point was systematically deleted in the matrix element evaluation. This means that an information carrying the data describing which points are significant, is also needed to be determined for each matrix element. This scheme was found to be very helpful because only a small fraction of grid points is involved for the integration purpoe, i.e., the XC-potentials at those points only are multiplied to the previously generated values and summed. Less than three minutes CPU time was needed for one iteration for Fe_9 cluster with a total of 1,302 grid points. A similar scheme was also used to generate the charge density at the grid points, i.e., values of $\chi_i(r_k)$ were pre-determined before the start of iteration cycle.

F. Self-Consistent Procedure

The calculation was started with the initial configuration of overlapping fitted atomic charge density and the numerical data of exchange-correlation potential V_{XC} at the gird points (V_{XC} was evaluated directly from the charge density generated). The charge density was generated from the well-documented Hartree-Fock atomic wave functions and the least-square fitting method was used to obtain the initial fitted atomic charge density.

During the iteration process, charge density for each representation R was obtained from the expression

$$\rho_R(\vec{r}) = \sum_{r=1}^{d(R)} \sum_{n=1}^{nocc} g_n \, |\psi_n^{(r)}|^2 \quad .$$

Occupancy of the eigenstates g_n was determined from T=0°K Fermi distribution function which gives the occupancy of 1 if that state lies below the Fermi level and 0 if it lies above. It can be shown rigorously that the energy levels generated from the LDA calculation satisfy the Fermi statistics.[60,61]

As has been discussed before, any single row only in a given irreducible representation needs to be considered in forming and diagonalizing the Hamiltonian matrix because of the degeneracy property. This means that identical wave function coefficients could be assumed for all the rows in a given representation if the basis functions are properly normalized. Proper normalization of the basis

functions to obtain identical eigenfunction coefficients is important because basis functions belonging to every row in a given representation should be used in generating the charge density, whereas the eigenfunctions are determined from any single row.

Although every degenerate eigenfunctions have to be used in generating the numerical charge density and therefore the XC-potential from it, any single row eigenfunctions only are needed when the integrated quantity from the charge density is generated such as $\vec{t}$ in the charge density fitting. Evaluation of $\vec{t}$ can be done by using analytical integrals and the original eigenfunctions, as has been discussed.

Iterative method which is the most conventional way of solving non-linear differential equations such as the Schrödinger equation has been employed to obtain the self-consistent solution.[62] In this method, the best possible estimate of the input potential is constructed out of the potentials from previous iterations. This potential is used to find new eigenfunctions and therefore a new potential. The most commonly used form of constructing the new potential,

$$V_{in}^{n} = (1 - f)\ V_{in}^{n-1} + f\ V_{out}^{n-1}$$

has been used in this work. Usually f is a very small positive constant less than 1.0. Generally f should become smaller to get convergence as the degree of freedom of a system is increased.

In the present calculation, we have tried the 'iteration cycle' scheme proposed recently.[63] In this scheme, the mixing factor f is not kept constant but is allowed to vary from iteration to iteration between a small and a large constant. This 'iteration cycle' scheme helped speed the converging process, but the difficulty involved in proper choice of the alternating factors still made this scheme very cumbersome to use systematically. In the process of iteration, we have found that the choice of two damping factors being used could be varied for faster convergence, especially at the final stage of convergence where very large factors could be used. We also experienced difficulty in getting convergence due to flipping of two competing levels near the Fermi energy. Instability of energy levels due to flipping tendency of the two levels is a well-known phenomenon in the LDA in contrast to the H-F method in which the levels have a tendency of not flipping from each other.[64] Incomplete self-interaction correction in the LDA potential form has been pointed out for this problem.

Such nature in LDA calculation makes the convergence rate very slow due to the necessity of having to use only very small damping factors, since large damping factors usually lead to wild oscillation of charge density and the eventual divergence especially in the early period of iteration.

In our calculation, we could reach steady state at about 10~20 iterations with damping factors of 0.04~0.08. At this stage, relative position of energy levels stayed fixed, and therefore the average magnetization number also. But convergence to absolutely self-

consistent solution became very slow after that as has been described in Ref. 63.

We have found that Fe_{15} cluster convergence is harder to get than that of the Fe_9 cluster as could be expected due to a larger degree of freedom in Fe_{15} basis set. At one stage of iteration process in Fe_{15} calculation, we had to impose degenerate occupancy to the flipping levels near the Fermi level. This constraint was removed after the two levels became sufficiently separated. Setting the convergence criterion in this type of calculation does not seem to be clear-cut. We checked the convergence rate of the exchange potential, the charge density fitting coefficients, and the total energy for signs of convergence.

We stopped the iterations when the energy level changes were less than 0.0002 Ryd and the total energy change less than 0.01 Ryd. Convergence rate of the charge density fitting coefficients could also be used for this purpose and all quantities checked showed a reasonably consistent trend in the convergence rate.

Because of the increasingly slow nature of convergence rate near the end of iteration, we sometimes experienced difficulty in getting perfect convergence but have found that the general features of cluster properties does not show any noticable difference through iteration at this final stage.

Equal fractional occupancy for degenerate Fermi level was imposed if that level happens to be partially occupied. This choice certainly preserves symmetry of clusters which is a necess ty in our calculation, but giving full occupancy of 1 to eigenfunctions belonging to some

arbitrary row and 0 for others in a given representation can create a symmetry problem in the calculation. If a calculation of better accuracy for such clusters were needed, our choice of equal fractional occupancy for degenerate Fermi level should be given another consideration since the symmetry lowering possibility such as the Jahn-Teller effect could be more realistic situation.[51] In our present calculation, we do not have sufficient accuracy to treat such problems and we intend to pursue more general features of cluster properties.

CHAPTER III.

RESULTS AND DISCUSSION

In this chapter, we discuss the systems studied in this work and the results obtained from the present method. We describe the cluster models in Section A and the energy levels for clusters Fe_9 and Fe_{15} is presented in Section B. Section C contains the discussion of density of states (DOS) obtained from the cluster energy levels and a comparison with the solid DOS is made. Spin densities at various locations in the cluster systems are discused in Section D, and the ionization potential obtained from the transition state calculation is presented in Section E. Finally, a brief discussion on the result obtained for the carbon impurity system is given in Section F.

A. Cluster Models

The first system we considered was Fe_7 atomic cluster with two different lattice spacings of 5.4 a.u. and 4.0 a.u. each. The atomic arrangement of this system is octahedral and corresponds to an atom and its first six nearest-neighbors in simple cubic lattice. Though iron is known to have BCC symmetry, this system was chosen for testing purposes in the preliminary stage of calculation. For this system only, Kubic Harmonic expansion techniques were used instead of the direct numerical evaluation approach for the exchange potential.

Our procedure was then applied to body-centered cubic (BCC) iron atomic clusters, first to Fe_9 cluster which corresponds to an atom and its eight first nearest-neighbors in BCC solid iron. To help study convergence of the cluster properties to those of solid, we then added six more atoms which corresponds to second nearest-neighbors. Though a comparison of cluster properties with those of bulk is one of the main objectives in this work, embedding conditions were not imposed and free clusters with open boundary only were considered. Geometrical arrangement of atoms for these custers and those for simple- and face-centered cubic symmetries are shown in Fig. III-1.

Lattice parameter for the clusters was put to 5.40 a.u. which roughly corresponds to the solid parameter. This gives the distance between the central and first nearest-neighbor to be about 4.68 a.u. This choice of lattice spacing is somewhat smaller than the number 5.4057 a.u. used in Ref. 6. The exchange-correlation potential of von

Barth-Hedin type[38] which has the abstract form of

$$V_{\sigma}^{XC} = A(\rho)\ (^{\rho}\sigma/\rho)^{1/3} + B(\rho)$$

was employed for this calculation. Parameters used in $A(\rho)$ and $B(\rho)$ can be found in Ref. 39. Results obtained from this potential could be directly compared with the band structure properties obtained using the same potential.[46] Although other types of local density form such as the Xα-type potential could also be used and compared with the relevant band structure calculations, it does not seem to alter the essential physical properties very much.

Although the study of cluster property was the main objective in this work, we also considered Fe_8C and $Fe_{14}C$ clusters, for which the central iron atom is replaced by a carbon atom. We have considered this system to prepare for future study of impurity containing systems, though other type of boundary condition is expected to be needed for this purpose.

Though we have considered only the simple cubic and body-centered cubic symmetry clusters in this study, our method is immediately extendable to systems which have face-centered cubic symmetry. For example, Ni_{13} and Ni_{19} clusters or Cu_{13} and Cu_{19} clusters could be directly handled with this method (Copper cluster calculation will need slight modification of the code, however, to adopt paramagnetic form of the exchange potential).

B. Energy Levels

The molecular orbital energy eigenvalues from the spin polarized calculations of Fe_9 and Fe_{15} clusters are shown in Figs. III-2 and -3, respectively. The values of several important quantities resulting from these energy levels are summarized in Table III-1, where they are compared with the results obtained from the MS-Xα method. Relevant quantities from the band structure calculation of iron using the VBH potential are also listed to see the convergence trend of cluster properties to those of bulk iron.

Because of the availability of results reported previously which were obtained using the MS-Xα method,[6] our results are compared with those results extensively. However, it should be noted that the local density functional used in MS-Xα is the Xα potential with $\alpha=0.71$.

Figure III-2 shows that our levels for Fe_9 cluster compares favorably with the MS-Xα energy levels. We have the same $3t_{iu}\uparrow$ level as the last occupied level with double electron occupancy. Also, the distribution of occupied and unoccupied levels for each representation is identical in both cases. Although the general features are identical, relative locations of the energy levels can be seen to be somewhat different. For example, the very large gap between occupied majority-spin d-manifold and the unoccupied d-character levels above them which existed in the MS-Xα result is found to not be as large in this case. Thus we have less ambiguity in defining the d-bandwidth due to this reason. This gap was maintained significantly large in Fe_{15}

cluster also in the MS-Xα result which led to an ambiguous determination of the d-bandwidth (see Table I of Ref. 6). As could be seen in Fig. III-3, this gap has almost disappeared for Fe_{15} levels in our case. The trend of convergence towards bulk bandwidths from Fe_9 to Fe_{15} is obvious from Table III-1. The present result can be seen to agree with most of the conclusions made in Ref. 6 and, in fact, provides even stronger support for them in many respects. We can summarize those aspects in the following categories. First, the occupied s-bandwidths for both spins are significantly larger in the present result. They are about 65% and 25% larger than the MS-Xα result for Fe_9 and Fe_{15} clusters, respectively. Therefore, more than 90% of the bulk bandwidths are obtained for Fe_{15} in the present case. Second, present occupied d-bandwidths are converging to those of bulk more uniformly. Though the majority-spin occupied widths are about the same magnitude as were obtained in Ref. 6, the minority-spin widths are larger in the present case. This makes the relative magnitude of the occupied d-widths for both spins to be very similar to those of bulk for both clusters. In Ref. 6, the minority-spin occupied d-widths were noticably small compared to its majority-spin counterpart, which probably is due to the use of Xα-potential (Xα-potential is known to produce too large exchange splitting). The present occupied d-bandwidths for Fe_{15} are also found to be more than 90% of the bulk widths. Third, the present full d-bandwidths are again larger than those reported in Ref. 6 and the cluster d-widths can be determined unambiguously. Determination of the d-bandwidths was not easy in the MS-Xα result and this led to ambiguous

and disputable d-bandwidths. Furthermore, in either choice of its determination, convergence to bulk d-widths could not be achieved satisfactorily in a quantitative sense. Present result shows that d-bandwidths are converging to those of bulk in an unambiguous and satisfactory manner. We also find that the level dispersion is significantly larger for the minority spin levels in agreement with band theory. Present full d-bandwidths for Fe_{15} are also found to be about 90% of those of bulk. We have discussed the convergence trend to bulk properties in terms of cluster bandwidths obtained from the energy levels and have found that all the major quantities for Fe_{15} are within 10% difference from those of bulk.

Another point which strongly supports the convergence property to bulk can be made from the positions of the sp-like levels. As is well known, transition metal band structure is characterized by the relatively narrow d-band overlapped by wide sp-band originating from the rather delocalized sp-electrons, with a possible hybridization of the two bands in the overlapping region. Energy levels in Figs. III-2 and III-3 show this characteristic very obviously if we regard present sp-levels as the precursor for sp-bands, e.g., relatively narrow and dense distribution of d-levels is overlapped by a broader and sparse distribution of predominantly sp-like levels for both spins. The a_{1g} and t_{1u} levels, which are the s- and p-type analogs are enveloping the whole d-manifold from both ends. The a_{2u} level located at the top region is mainly of s-character. Also coinciding with band theory, our sp-level exchange splittings are a lot smaller than those of the d-levels. Our

value of exchange splitting 0.5 eV for the a_{1g} level at the bottom lies in the middle of the s-band range in the band-theory, which is 0.16~0.85eV.

Because of the difference in method and the difference in the adopted local density functional form for exchange potential, some of our results are significantly different from those of Ref. 6, especially the Fe_{15} energy level distribution. Considering that the muffin-tin potential is used in MS-Xα method, we can expect that rather delocalized sp-like levels to exhibit more difference in the two methods due to the constant potential approximation made outside the muffin-tin region. On the other hand, relative locations of the rather localized d-like levels are not expected to be very different in the results from both methods. In fact, we find large differences in the relative positions of sp-like levels from those of Ref. 6, providing an even stronger symptom of the sp-band overlapping of the d-band character. This fact shows that by removing the muffin-tin approximation, convergence trend to bulk properties is manifested even more favorably.

The general feature of our levels shows that exchange splitting of the levels are reduced compared to the MS-Xα result. This is seen by shifting of the whole majority-spin levels closer to the Fermi level and is consistent with the fact that the Xα-potential usually generates larger exchange splitting than it should.

Our occupied level configuration for Fe_{15} was found to be slightly different from that of Ref. 6. We find $4a_{1g}\uparrow$ level as the non-degenerate Fermi level and the $6e_g\uparrow$ level fully occupied. Instead the

$4t_{1u}{}^{\downarrow}$ level is not occupied anymore. These differences result in the relatively large magneton number for the Fe_{15} cluster, which is 2.9 net spin per atom compared to 2.7 reported in Ref. 6. This shows that convergence of the magnetron number of clusters to that of bulk is not as obvious as was pointed out in Ref. 6. We will discuss this situation further in connection with the spin density problem later.

We have discussed the energy levels and the properties obtained from them in the present work in comparison with the MS-Xα result. Overall features of the present result indicate that our result exhibits the convergence trend of the cluster properties to those of bulk more unambiguously and convincingly. Comparison of the results for Fe_9 and Fe_{15} indicate that the bandwidths properties are extremely rapidly converging to those of bulk iron. The removal of muffin-tin approximation also led to the shift of sp-like levels and contributed to exhibiting clearly the s-band overlap feature of the bulk. These are indirect but obvious indications that the short-range atomic interactions are mostly responsible for determining the bulk properties.

An objection to the above point of view was made recently which may be worth mentioning.[7] Those authors who used the H-F method for their Copper cluster calculations reported that they couldn't observe the sp-band overlapping feature even for Cu_{13}. Their result showed that the sp-levels are just beginning to overlap with the d-levels for Cu_{13} and claimed that such a feature observed in the MS-Xα levels is a spurious result due to the incomplete self-interaction correction defect of local density functionals. Their argument was based on the fact that the

self-interaction correction is more significant for finite systems and that the s-level correction term could be very different from that of d-level. However, other authors later showed that such differences in the correction term is almost negligible for Cu_9 cluster already.[65] Since the sp-band extends over 10 eV range for both spins and since it envelops the d-bands so completely in the present case, it seems that more than 5 eV self-interaction correction difference is needed to claim its spuriousness, which is very unlikely.

C. Density of States

Though lots of quantitative evidences showing the convergence property of clusters to bulk have been discussed in the previous Section, direct comparison of the density of states (DOS) profiles could be more convincing.

The quantity which involves least ambiguity will be the integrated DOS, N(E), which is defined to be the number of states per atom with energies less than or equal to E. Specifically,

$$N(E) = \sum_i g_i \, \theta(E - E_i)$$

in which g_i is the degeneracy of the state whose energy is E_i and θ indicates step-function. This quantity is shown in Fig. III-4 for the Fe_{15} cluster for both majority and minority spins. Figure III-5 shows the quantity when both spins were added, e.g., total integrated DOS. The result obtained from the band calculation of Ref. 46 are presented for comparison in both Figures. The zero of energy has been taken as the Fermi energy for this purpose.

It will be seen that there is a substantial degree of general agreement between the cluster and bulk results in regard to the position of regions of relative flatness and of rapid increase. Because of the large magneton number difference between the two systems, Fig. III-4 shows large gap near the Fermi energy. In Fig. III-5, where this difference is not manifested anymore, the relative similarity between the

two quantities is remarkable. This indicates that this relatively small Fe_{15} cluster already possesses an energy level distribution which resembles remarkably well that of bulk iron, supporting the "invariance property" of DOS discussed in Chapter I. The reasonable agreement obtained for the integrated DOS suggests that DOS itself could also have reasonable resemblance, if we manipulate the levels properly to generate approximate DOS.

We have generated the DOS profile for clusters by replacing each enegy level by a Gassian of width parameter 0.2 eV, the same parameter as was used in Ref. 6. Using this scheme, the DOS per atom can be written as

$$G(E) = \left(\frac{1}{N_A \cdot \sqrt{2\pi} \cdot \sigma}\right) \sum_i g_i e^{-(E-E_i)^2/2\sigma^2}$$

in which N_A is the number of atoms in the cluster, g_i is the degeneracy of level E_i, and σ is the width parameter.

Result of such broadening of each level can be shown to be identical to smoothening the original step-function like integrated DOS, larger σ corresponding to more severe smoothening. Choice of σ = 0.2 eV was found to be reasonable, the resulting integrated DOS being moderately smoothening the original integrated DOS. The physical implication of such broadening is equivalent to embedding the cluster in a periodic lattice, but only approximately. Such scheme of broadening each level by a uniform factor has the defect of disregarding the difference between the localized d-levels and the relatively delocalized

states such as predominantly sp-like levels. It would be desirable to assign broader Gaussians for delocalized states, which has not been done in this work.

The resulting DOS generated using this scheme is shown in Figs. III-6, -7, and -8. Figure III-6 shows the total, majority- and minority-spin DOS of the Fe_9 cluster in a single figure. It is obvious that it does not resemble those of bulk at all. But the minority-spin and total DOS parts begin to show slight signs of bulk property already.

In Fig. III-7, the majority- and minority-spin DOS's of the Fe_{15} cluster and bulk are superposed for direct comparison. The degree of similarity is truly remarkable obviously. It should be noted that the two peaks on the far left and far right for majority-spin DOS are coming from the delocalized sp-character levels. These are the spurious peaks resulting from the use of a same broadening factor for all the levels. The two peaks on the far left and hidden peaks on the far right for the minority-spin DOS are of the same spurious nature. Comparison of Fig. III-7 with Fig. 7 of Ref. 6 shows that present result demonstrates the sp-band overlapping character more explicitly. Furthermore, present result describes the majority-spin DOS shape near the Fermi level a lot better than before. This is due to the absence of large gap of energy levels which was discussed before. Present result also represents three distinct peaks manifested in band majority-spin DOS better by having a larger gap between peaks 2 and 3 in Fig. 7 of Ref. 6. Another noticable feature of the present majority-spin DOS is that the highest peak part of the band DOS is represented by splitted two peaks. On the other

hand, peak 3 of Fig. 8 of Ref. 6 which is the central peak of band majority-spin DOS with some structure is represented by a single structureless peak in our result as it has been in the MS-Xα result.

The minority-spin DOS in Fig. III-7 shows that three distinct peaks of band minority-spin DOS are also well represented in this work as it has been in Ref. 6. We have a local minimum at the Fermi level and another local minimum at about 2 eV below. Better representation of band DOS by Fe_{15} DOS of present work than by that of Ref. 6 can be seen convincingly when we check the overall relative postions of peaks and valleys for both majority- and minority-spin DOS. This result could be related partly to the use of different exchange potentials in the two calculations since Xα-potential is generally known to produce relatively large exchange splitting.

To prove the similarity property between the cluster and bulk DOS further, we also plotted the total DOS of the Fe_{15} cluster and iron solid. Figure III-8 shows the two quantities in superimposed form again for direct comparison. Except for the two spurious peaks on the left and others on the right, there is again remarkable resemblance between the two results. Total number of major peaks as well as the positions of local minimums of band total DOS are almost perfectly represented in the Fe_{15} total DOS already.

Remarkable resemblance between the approximate DOS generated by broadening each energy level of Fe_{15} by Gaussian type functions and the bulk DOS generated by band structure calculations has been discussed in this Section. First doubt we can have is such a close similarity it-

self. Considering that most of the atoms in Fe_{15} are surface-like atoms, we could expect our DOS to be more similar to the surface DOS than the bulk DOS, and surface DOS is known to be very different from bulk DOS. We could not think of any convincing explanations for this question. But one point about this situation can be made clear, which is the fact that the ligand atoms in Fe_{15} which is still a relatively small cluster, are not in similar environment at all as the atoms on the surface of a solid, e.g., they could have very different local DOS. What we could get for the DOS using the energy levels obtained from the short-range atomic interactions of such a miniature solid like Fe_{15} seems to show a lot of infinite solid character already.

D. Spin-Density and Magneton Number

Spin density distribution in space is known to be a very sensitive quantity which depends a lot on the choice of exchange potential used.[46]

One of the characteristic features of spin density in iron and some other transition metal solid is the appearance of weak but significantly large regions of negative polarization (e.g., minority spin dominated regions) at the interatomic space region.[15] Such negative polarization also occurs at the nucleus site where it is extended to extremely small region around the nucleus, resulting in a negative hyperfine field at the nucleus site. This is one of the important properties of some transition metals. Other than the above described regions, the space is composed of approximate spherically symmetric regions of strong pisitive polarization centered on each nuclei.

It was reported in Ref. 6 that {100} plane of Fe_{15} which contains four atoms of the first shell atoms already shows the negative polarization character described above. We have plotted spin density contour on several planes to prove this feature and other features and we have found the most serious difference with the results of Ref. 6 in this property. Very surprisingly, our central atom was found to be dominated by minority spin electrons. This situation was more profound for Fe_9 cluster and was alleviated a lot for Fe_{15}. The value of approximate net spin number for this central atom, determined by rough geometrical region integration was -0.70 and -0.10 for Fe_9 and Fe_{15} respectively. This is a quite surprising result considering that iron is a typical

ferromagnet.

Contour plot of spin density of {100} plane showed that we neither have negative polarization region on this surface in Fe_{15} at all. However, for Fe_9, some region of negative polarization appeared at the central region of {100} plane. To see the effect coming from the difference in the configuration of occupation numbers in the two results, we also tried the occupation number configuration reported in Ref. 6 in generating spin density. We have found that even with such change, the reported spin density map could not be reproduced exactly. However, a small region of negative polarization at the center of the plane could be observed in this case. This situation is somewhat embarassing since the eignefunctions for each relevant level are not expected to be very different, although a significant difference could be expected for delocalized orbitals due to the muffin-tin approximation in MS-Xα. But considering that the magnitude of negative polarization is very small, a small difference in eigenfunctions may be enough to cause such difference.

However, the most surprising outcome of present calculation should be the minority-spin dominating situation for the central atom. In MS-Xα result of Ref. 6, the central atom was reported to have a net spin number of +1.15 for Fe_{15}, a small but definitely a positive quantity. The reason for such a small magneton number was analyzed to be due to the influx of minority-spin electrons to the central site, resulting in more total number of valence electrons for the central atom. We also observed such trend for the Fe_9 cluster which was manifested in

relatively lifted core energy levels of the central atom. Core energy levels for Fe_9 and Fe_{15} designated with each shell index are presented in Table III-2. Though the central atom for Fe_9 was found to have more electrons than others, the situation for Fe_{15} was different. The Fe_{15} cluster core level study shows that core levels have become deeper than those of other atoms, indicating the possibility of outward flow of electrons to ligand atoms. This is contrary to the findings of MS-Xα calculation, and also opposite to the situation in Fe_9.

Spin density around the central atom was also found to be very anisotropic. Along the [111]-direction, a local maximum (in magnitude) of negative polarization was found at about 0.5 a.u. and the range of negative polarization was found to reach up to about 2.3 a.u. On the other hand, it was limited to a very small distance from the center along [100]-direction.

Contact spin density, which is the spin density at nucleus site is another quantity of interest. This quantity was, however, found to have a difference of over 50% when different types of local density potential were used in the LCGO method band calculation.[46] In this band calculation, contact spin densities of -0.406 and -0.655 were obtained for VBH and Kohn-Sham potentials respectively, whereas the experimental value was -0.647. On the other hand, MS-Xα calculation of Fe_{15} with parameter $\alpha = 0.71$ was reported to produce -1.05, -0.77, and -0.55 for the central, firts- and second-shell atoms respectively. Furthermore, comparison of relative contributions from each orbital showed that the ligand cluster atoms are behaving quite similar to bulk atoms as far as

this quantity is concerned (especially the first-shell atoms). This is quite surprising since the ligand atoms have very large mageton number compared to the bulk atom.

The contact spin densities in our calculation shows somewhat reverse trend from those of MS-Xα calculation, giving -0.08, -0.24, and -0.40 for the central, first- and second-shell atoms for Fe_{15}. For Fe_9, the central- and first-shell atoms were found to have -0.71 and +0.24 respectively. Obviously, there is a large difference in qualitative as well as in quantitative character between the two clusters Fe_9 and Fe_{15}. Open boundary condition for Fe_9 seems to result in large abnormality not only for the central atom but also for the ligand atoms. Compared to Fe_9, the Fe_{15} cluster obviously have converged to bulk quite significantly. Though the central atom still shows a sign of substantial abnormality, ligand atoms for Fe_{15} look quite similar to bulk atoms.

Because of such abnormal nature of the central atom in both clusters, it is suggested that such open boundary clusters are not expected to be a good model for impurities in a solid. Convergence trend of average magneton number to that of bulk as the cluster size becomes large could not be confirmed due to this reason also. For Fe_9, abnormally strong domination by minority-spin electrons at the central site gives a small average spin number of 2.89. Assuming that the central atom has spin number of -0.70, a ligand atom is found to have a spin number of 3.34 for this Fe_9 cluster. For Fe_{15}, assuming a net spin number of -0.10 for the central atom, a net spin number of 3.15 for the

ligand atoms is obtained. To be exact, the second shell atoms are expected to have slightly larger spin number than the first shell atoms. Though we have not evaluated such quantities, estimated average values of 3.10 and 3.20 for the first- and second-shell atoms can be guessed from the known information.

Average net spin numbers for the surface like ligand atoms, 3.34 and 3.15 for Fe_9 and Fe_{15} respectively, are reasonably consistent with the value of 3.0 Bohr magnetons for the solid surface atom obtained from surface calculation.[15] We can expect that the ligand atoms for such small clusters are in a more severe "surface" situation than the solid surface itself. As the size of the cluster becomes larger, it is expected that the net spin number of cluster surface atoms to approach that of the solid surface atoms. In this respect, average spin numbers in Ref. 6, wihch are 2.71 and 2.80 for the first- and second-shell atoms in Fe_{15}, are quite inconsistent with both this work and Ref. 15.

As have been mentioned earlier, preliminary calculations using the Kubic Harmonic expansion method was also made for Fe_7 clusters at two different atomic spacings 5.4 a.u. and 4.0 a.u. The atoms in this cluster were arranged in an octahedral geometry. Average moments obtained were 3.7 net spin per atom for the 5.4 a.u. spacing and 3.0 for the 4.0 a.u. spacing. Assuming that widely separated iron atoms have magneton number of 4.0 μ_B belonging to the iron atom itself, our value of 3.7 for the large 5.4 a.u. spacing seems reasonable. As the atoms were squeezed further to 4.0 a.u. spacing, broadening of energy levels resulted in a smaller magneton number as was expected.

E. Transition State and Ionization Potential

In the H-F method, orbital energy ε_i^{HF} has some meaning in relation to the total energy of a system by Koopman's Theorem, which says that

$$\varepsilon_i^{HF} = E^{HF}(n_i = 1) - E^{HF}(n_i = 0) \quad .$$

The first term on the right is the total energy of a system and the second term is the total energy of ion with the i^{th} electron removed without allowing all other orbitals to relax. Therefore, the eigenvalue of the last occupied level is an approximate (although not exact) ionization potential (I.P.) in magnitude.

On the other hand, in the LDA method, orbital energies are related to total energy as $\varepsilon_i^{LDA} = \partial E/\partial n_i$ and have less physical significance than the H-F eigenvalues in this respect. One obvious way of calculating the energy differences involved in optical transitions in LDA method is to make two separate calculations, one for a system itself and another for the system after the transition has occurred. Though this procedure is straightforward and true in theory, usual inaccurate evaluation of total energy for a system causes practical difficulty very often. Furthermore, it is time-consuming and laborious to make two separate calculations.

An alternative Transition State procedure was proposed by Slater to facilitate such calculation.[18,66] The basic principles behind this method are the recognition that occupation number n_i could be continuous

between 0 and 1 in LDA and that the total energy is mainly a function of linear and quadratic term of n_i's. (If only a linear term exists, then $\varepsilon_i^{HF} = \varepsilon_i^{LDA}$ can be shown to hold.) A much smaller but finite third order term was also found to exist but is neglected in this method.

If we take up to quadratic expansion of n_i for E, then

$$E(n_i \ldots n_i \ldots) = E|_{n_i = \frac{1}{2}} + (n_i - \tfrac{1}{2}) \frac{\partial E}{\partial n_i}|_{n_i = \frac{1}{2}} + \frac{1}{2} (n_i - \tfrac{1}{2})^2 \frac{\partial^2 E}{\partial n_i^2}|_{n_i = \frac{1}{2}}$$

holds if the expansion is done with $n_i = \frac{1}{2}$ (and all other n's unchanged) as the reference state. Then

$$E|_{n_i=1} - E|_{n_i=0} = \frac{\partial E}{\partial n_i}|_{n_i = \frac{1}{2}}$$

can be obtained using the above expansion form. The left hand side is the ionization energy expression and the right hand side is the i^{th} energy eigenvalue obtained from the Transition State calculation.

Therefore, if a calculation is made with non-integer occupation number of $\frac{1}{2}$ for the i^{th} state, ε_i is itself the ionization energy of the i^{th} electron. Although this example considered specifically ionization energy, it is obvious that it can be generalized to any arbitrary optical transition from state $i \rightarrow j$. In this case, the difference of eigenvalues $|\varepsilon_i - \varepsilon_j|$ equals the excitation energy, if a Transition State calculation is made with $n_i = n_j = \frac{1}{2}$ constraint.

The transition state which is considered here is obviously not a physical state but a fictitious state which is the average of initial

and final state. With proper consideration of initial and final state for any excitation problem, such scheme has been shown to be quite powerful in many examples of previous calculations.[67] This scheme can also be used for magnetic excitation problems in a ferromagnetic material and the energy difference calculated for a local spin flip using this method can be used for estimating the Curie temperature.[18] Estimation of the Curie temperature from first-principles calculation could be quite an achievement, but we have found that open cluster model cannot be used for such purpose due to already discussed abnormality of the central atom.

However, we used this scheme to determine the ionization potential of Fe_9 cluster. This calculation can be done by simply removing half an electron from the finally occupied level. This calculation, which was also spin-polarized, gave 0.378 Ryd (5.2 eV). This quantity is reasonably close to recent experimental value of 5.3~5.6 eV[72] considering the uncertain geometry of the experimental Fe_9 cluster. Since the doubling grid we used was found to reduce the matrix element value by about 3% generally, we expect our result can be within the experimental range if a finer grid is used.

To test the reliability of total energy calculated, ionization potential was determined also from the total energy differences. For the Fe_9 system,

$$< E >_z = -22686.11 \text{ Ryd}$$

$$< E >_{z-1} = -22685.90 \text{ Ryd}$$

were obtained from two separate calculations of a regular system and of a system with one electron removed. Therefore we find 0.21 Ryd (2.9 eV) for the ionization potential by this procedure, which is obviously far off from the experimental value range. This and other informations we checked indicate that the total energy obtained by present method is not accurate enough to give good result on such sensitive quantities. It was found that the charge density fitting is most responsible for the error involved in the total energy calculation.

F. Carbon Impurity Systems

From the analysis of pure iron clusters, it was found that the central atom in such small clusters does not resemble a typical bulk atom at all. This indicates that the open boundary condition for such small clusters is not a good model for describing impurity problems in solids. In fact, it was reported that such small clusters are not very effective for impurity problems even when some embedding potential was imposed.[68]

Carbon impurity in iron systems was considered in our present work only to prepare for more realistic work in the future, e.g., with a possible embedding potential. The central atom in the Fe_9 and Fe_{15} clusters were replaced by a carbon atom and self-consistent, spin-polarized solutions were obtained following exactly the same procedure as was used for the pure iron clusters.

The basic trend of the physical situation was found to be consistent with those of pure iron clusters. The central atom was dominated again by minority-spin electrons for Fe_8C and the contact spin density for the ligand iron atoms was found to be a positive quantity +0.47 as it has been for Fe_9. Such abnormality for the ligand atoms already implies that the central carbon atom is not placed in the desired environment and is unduly perturbed also. The contact spin density for the carbon site was +0.22 and the magneton number for the ligand iron atoms was found to be about 3.5 μ_B for Fe_8C.

For $Fe_{14}C$, the central carbon atom was, however, found to have slightly positive polarization. The contact spin densities of the central-, first-, and second-shell atoms were +0.40, -0.07, and -0.45 respectively. The DOS profile for $Fe_{14}C$ generated by the same scheme as before is shown in Fig. III-9. Though many of the features discussed on Fe_{15} DOS is still found, the whole structure itself is obviously vastly different from that of the pure iron cluster. It is surprising that the seemingly minor perturbation of a carbon atom could destroy the nice similarity between the cluster and bulk DOS to such an extent. The overlapping nature of sp- and d-band is also found in this case and the minority-spin DOS seems to be less perturbed than the majority-spin part. Another peak appearing on the left side and heavily perturbed shape for the majority-spin DOS is probably due to carbon sp-level presence. The breakdown of good DOS similarity between the cluster and bulk due to carbon atom replacement in $Fe_{14}C$ may be an indication that such similarity obtained for Fe_{15} DOS is not an accidental consequence.

Replacement of the central iron atom by a carbon atom seems to reduce negative polarization trend on that site. The magnitude of negative polarization was smaller for Fe_8C than it was for Fe_9 and it could recover slightly positive polarization for $Fe_{14}C$ though the Fe_{15} central atom was still slightly minority-spin dominated. The contact spin densities show that the first-shell atoms were perturbed more than before but the secnod-shell atoms have not been perturbed much in this case. This may indicate that the existence of a carbon atom instead of an iron atom at the center only weakly influences the second nearest-

neighbors. Average magneton number for the ligand atoms in $Fe_{14}C$ is about 3.3 μ_B which seems reasonable.

IV. CONCLUSIONS

Self-consistent spin-polarized calculations were made for small iron clusters Fe_7, Fe_9, and Fe_{15}. Similar calculations were made for Fe_8C and $Fe_{14}C$ in which the central atoms were carbon atoms instead of iron atoms, to prepare for impurity system studies.

Our method which does analytical charge density fitting for the Coulomb potential as the only approximation for evaluating the matrix elements is regarded to be a more accurate approach than any other methods used before in dealing with large atomic clusters.

The overall features we could obtain for such 'miniature solid' Fe_{15}, containing only the first and second nearest-neighbors arranged in solid BCC geometry are found to be remarkably close to those of bulk already. The full d-bandwidths as well as the occupied portions are a lot wider in the present result for Fe_{15} than the values obtained previously using the MS-Xα method and are within 10% difference from the relevant bulk quantities. Furthermore, present DOS profiles for Fe_{15} are virtually identical in characteristic shape with those of bulk, which means that not only the qunatitative features but also the qualitative features are well represented already. Another remarkable feature of the present result is the obvious overlapping of the sp-band with the d-band, which is even more explicitly manifested in this work than was shown in Ref. 6. On the other hand, hardly any features resembling the bulk could be noticed for the Fe_9 result, though there are some early symptoms of similarity.

That the DOS profile for Fe_{15} already represents the bulk character is particularly surprising since such a small cluster with open boundary is expected to have quite a significant amount of surface effect. What we find from the present calculation is that the basic characteristics of bulk DOS is somehow manifested even for such small systems which have relatively large surface effect. To what extent the variances observed in the two DOS profiles are due to such size effect is not clear however and should be considered more carefully, since most of the previous calculations referred to size effect whenever it could not find any reasonable relevance for the physical properties between the two systems, bulk and cluster. Our calculation, which is expected to be the most accurate work done so far on such systems, seems to exhibit such similarity more extensively than the previous less accurate calculations. It looks as if better similarity in physical properties can be obtained as the calculation becomes more accurate. It will be interesting to have the result for the Fe_{27} cluster, which has another shell added to Fe_{15}, to see the relative importance of the surface effect for such small clusters.

Although we could obtain superior result compared to Ref. 6 as far as the DOS similarity is concerned, we failed to observe the bulk-like spin density distribution at the interatomic regions (specifically [100] plane for Fe_{15}). Furthermore, the central atomic site was found to have a tendency to become negatively polarized. This was obvious in Fe_9 for which the central site was completely dominated by minority-spin electrons. However, for Fe_{15}, the central site was almost neutral

showing the trend of becoming positively polarized as the cluster size becomes large. Although the MS-Xα calculation also showed such trend of minority-spin electron flow to the central site, present work seems to show an even stronger trend for such flow. It is not clear at this time why such an unexpected situation develops although one explanation was suggested in Ref. 6. The more extended nature in space of the minority-spin orbitals could be an explanation also, providing accumulated minority-spin electron contributions from the ligand atoms to the central site.

The slow convergence of the central atom to a typical bulk atom for even very large clusters was reported and it is generally accepted at present that the central atom is not like the bulk atom for small clusters.[68,71] The convergence to bulk of the central atom for larger clusters is expected to be obtained according to a theorem by von Laue,[9] which states that the local density of states becomes approximately independent of the form of the boundary condition at distances from the boundary greater than a characteristic length inversely proportional to the wave number. Considering that the Fe_{15} cluster has only two ligand shells, it is expected that charge density distribution around the central site could hardly resmeble that of bulk according to the above theorem. In this respect, it is hard to believe that the spin density resembles that of bulk as was reported in Ref. 6 for such small clusters with open boundary.

Present work seems to indicate that a good similarity to bulk DOS could be obtained from such 'miniature solid' even though the charge and

spin density around the central site are extremely perturbed. The central atom for such small clusters should be very vulnerable since it has to adopt all the combined changes of the ligand 'surface-like' atoms. Even small changes of the ligand atoms could cause significant influence on the central atom when they are summed up. We tend to give up pursuing charge and spin density similarity with the bulk due to these reasons. Though it is not expected to be an effective model for realistic impurity problem, carbon impurity in the iron cluster with open boundary was also studied in this work. The good resemblance with bulk DOS is lost significantly for $Fe_{14}C$, and it seems the presence of the carbon impurity is almost ignored already by the second shell atoms. But we conclude that impurity calculations should not be done unless cluster size becomes significantly large or a satisfactory embedding scheme is imposed on small clusters.

The consequences of the present calculation could be checked for consistency using other systems such as Ni_{13} and Ni_{19}. Convergence trend of the central atom's charge and spin density to those of bulk could also be studied by extending the cluster size even larger (Fe_{27} for example), as a next step of calculation.

REFERENCES

1. V. Heine, Solid State Physics 35, 1 (1980); also D. W. Bullet, ibid 35, 129 (1980).

2. J. Friedel, Adv. Phys. 3, 446 (1954).

3. R. Nathans, M. T. Pigott, and C. G. Shull, J. Phys. Chem. Solids 6, 38 (1958).

4. J. E. Inglesfield, J. Phys. F2, 898 (1972); J. E. Inglesfield, J. Phys. C 4, L14 (1971).

5. R. L. Jacobs, J. Phys. F 3, L166 (1973).

6. C. Y. Yang, K. H. Johnson, D.R. Salahub, J. Kaspar, and R. P. Messmer, Phys. Rev. B 24, 5673 (1981).

7. J. Demuynck, M. M. Rohmer, A. Strich, and A. Veillard, J. Chem. Phys. 75, 3443 (1981).

8. K. H. Johnson, D. D. Vvedensky, and R. P. Messmer, Phys. Rev. B 19, 1519 (1979).

9. H. von Laue, Ann. Phys. 44, 1197 (1914).

10. J. C. Phillips, Phys. Today, February (1982).

11. H. A. Mook, J. W. Lynn, and R. M. Nicklow, Phys. Rev. Lett. 30, 556 (1973).

12. J. W. Lynn, Phys. Rev. B 11, 2624 (1975).

13. D. G. Westlake, C. B. Satterthwaite, and J. H. Weaver, Phys. Today, November (1978).

14. C. Demangeat, F. Gauthier, and J. C. Parlebas, J. Phys. F 8, 1879 (1978).

15. C. S. Wang and A. J. Freeman, Phys. Rev. B 19, 793 and 4930 (1979) and JMMM 15, 869 (1980).

16. R. P. Messmer, S. K. Knudson, K. H. Johnson, J. B. Diamond, and C. Y. Yang, Phys. Rev. B 13, 1369 (1976).

17. J. C. Slater, K. H. Johnson, Phys. Today, October (1974).

18. J. C. Slater and K. H. Johnson, Phys. Rev. B 5, 844 (1972); K. H. Johnson and F. C. Smith, Jr., Phys. Rev. B 5, 831 (1972).

19. D. E. Ellis and G. S. Painter, Phys. Rev., B 2, 2887 (1970).

20. E. J. Baerends, D. E. Ellis, and P. Ros, Chem. Phys. 2, 41 (1973).

21. B. Delley and D. E. Ellis, J. Chem. Phys. 76, 1949 (1982), also F. W. Averill and D. E. Ellis, J. Chem. Phys. 59, 6412 (1973).

22. C. B. Haselgrove, Math. Comput. 15, 323 (1961).

23. G. A. Benesh and D. E. Ellis, Phys. Rev. B 24, 1603 (1981).

24. B. Lindgren and D. E. Ellis, Phys. Rev. B 26, 636 (1982).

25. H. Sambe and R. H. Felton, J. Chem. Phys. 62, 1122 (1975).

26. B. I. Dunlap, J. W. D. Connolly, and J. R. Sabin, J. Chem. Phys. 71, 3396 (1979).

27. B. I. Dunlap, J. W. D. Connolly, and J. R. Sabin, J. Chem. Phys. 71, 4993 (1979).

28. E. Clementi, D. R. Davis, J. Comp. Phys. 2, 223 (1967).

29. R. C. Baetzold, J. Chem. Phys. 55, 4355, 4363 (1971); ibid. 62, 1513 (1975).

30. J. Kondo, Solid State Phys. 23, (1969).

31. W. G. Richards and J. A. Horsley, Oxford Science Research Papers 4, Clarendon Press, Oxford (1970).

32. E. Hückel, Z. Phys. 70, 204 (1931), 72, 310 (1932).

33. R. Hoffmann, J. Chem. Phys. 39, 1397, 40, 2047 (1964).

34. R. S. Mulliken, J. Chem. Phys. 46, 497 (1949).

35. J. C. Slater, Phys. Rev. 81, 385 (1951).

36. P. Hohenberg and W. Kohn, Phys. Rev. B 136, 864 (1964).

37. W. Kohn and L. J. Sham, Phys. Rev. A140, 1133 (1965).

38. U. von Barth and L. Hedin, J. Phys. C5, 1629 (1972).

39. A. K. Rajagopal, S. P. Singhal and J. Kimball (unpublished) as quoted by A. K. Rajagopal in Advances in Chemical Physics 41, 59 (Wiley, New York, (1979)).

40. M. L. Cohen and V. Heine, Solid State Phys. 24, 1 (1970).

41. J. C. Slater and G. F. Koster, Phys. Rev. 94, 1498 (1954).

42. S. H. Lamson and R. P. Messmer, Chem. Phys. Lett. 98, 72 (1983).

43. G. B. Bachelet, D. R. Hamann and M. Schlüter, Phys. Rev. B 26, 4199 (1982).

44. M. T. Yin, M. L. Cohen, Phys. Rev. B 25, 7403 (1982).

45. F. Bloch, Z. Phys. 52, 555 (1928).

46. J. Callaway and C. S. Wang, Phys. Rev. 16, 2095 (1977), also C. S. Wang and J. Callaway, Comp. Phys. Comm. 14, 327 (1978).

47. E. E. Lafon and C. C. Lin, Phys. Rev. 152, 579 (1966).

48. S. F. Boys, Proc. Roy. Soc. A 200, 542 (1950).

49. J. Callaway, Energy Band Theory, Academic Press, New York, (1964).

50. J. F. Cornwell, Group Theory and Elec. Energy Band in Solids, North-Holland Pub. Co., Netherlands (1969).

51. J. Callaway, Quantum Theory of the Solid State, Academic Press, New York (1976).

52. A. J. H. Wachters, J. Chem. Phys. 52, 1033 (1970).

53. B. Delley, D. E. Ellis, and A. J. Freeman, JMMM 30, 71 (1982).

54. D. Pines, Solid State Phys. 1, 367 (1955).

55. G. S. Painter, A. W. Averill, Phys. Rev. B 26, 1781 (1982).

56. J. W. Mintmire and B. I. Dunlap, Phys. Rev. A 25, 251 (1982).

57. F. C. von der Lage and H. Bethe, Phys. Rev. 71, 612 (1947)

58. R. Prasad and A. Bansil, Phys. Rev. B 21, 496 (1980) also W. R. Fehlner and S. H. Vosko, Can. J. Phys. 54, 2159 (1976).

59. M. Tinkham, Group Theory and Quantum Mechanics, McGraw-Hill, New York (1964) also M. Hamermesh, Group Theory, Addison-Wesley, Reading, Massachusetts.

60. J. C. Slater, Adv. in Quantum Chem. 6, 1 (1972).

61. J. Callaway and N. H. March (preprint).

62. D. R. Hartree, The Calculations of Atomic Structures, Wiley, New York (1955).

63. P. H. Dedericks and R. Zeller, Phys. Rev. B 28, 5462 (1983).

64. B. I. Dunlap, Phys. Rev. A 25, 2847 (1982).

65. D. Post and E. J. Baerends, Chem. Phys. Lett. 86, 176 (1982).

66. J. C. Slater, Quantum Theory of Molecules and Solids, Vol. 4, McGraw-Hill, New York (1974).

67. V. Gubanov and D. E. Ellis, Phys. Rev. Lett. 44, 1633 (1980).

68. B. Delley, D. E. Ellis, A. J. Freeman, E. J. Baerends, and D. Post, Phys. Rev. B 27, 2132 (1983).

69. R. Podloucky, R. Zeller, and P. H. Dederichs, Phys. Rev. B 22, 5777 (1980).

70. R. Haydock, Solid State Phys. 35, 216 (1980).

71. A. Hintermann and M. Manninen, Phys. Rev. B 27, 7262 (1983).

72. E. A. Rohlfing, D. M. Cox and A. Kalder, Chem. Phys. Lett. 99, 161 (1983).

Table III-1

Comparison of properties of iron clusters with those of bulk iron (eneriges in eV)

	Fe_9		Fe_{15}		Bulk
	MS-X_α	present	MS-X_α	present	Ref. 46
$(n\uparrow-n\downarrow)/N$	2.89	2.89	2.67	2.93	2.16
Occupied s-band ($\uparrow$)	4.7	6.7[a]	6.2	7.7[a]	8.20[i]
width ($\downarrow$)	3.7	6.3[a]	5.4	7.2[a]	8.03[i]
Occupied d-band ($\uparrow$)	3.8	3.8[b]	4.5	4.4[e]	4.75[j]
width($\downarrow$)	1.5	2.8[b]	2.9	3.3[e]	3.60[j]
Total d-band ($\uparrow$)	2.4	2.8[c]4.4[d]	(2.9)4.5	4.7[f]	5.13[k]
width ($\downarrow$)	2.8	4.0	(4.3)4.5	5.3[g]	6.12[k]
Range of Exchange Splitting (d)	1.8-3.2	0.7-3.1	1.2-3.2	1.0-2.7	1.1-2.2
Average Exchange Splitting (d)	2.7	2.3	2.5	2.4	
Exchange Splitting (sp)	1.0	0.4[h]	0.8	0.5[h]	0.16-0.85

a ; ε_F-$1a_{1g}$ b ; ε_F-$1t_{2g}$ c ; $3e_g$-$1t_{2g}$ d ; $5t_{2g}$-$1t_{2g}$

e ; ε_F-$1e_g$ f ; $7t_{2g}$-$1e_g$ g ; $3t_{1g}$-$1e_g$ h ; $1a_{1g\uparrow}$-$1a_{1g\downarrow}$

i ; ε_F-Γ_1 j ; ε_F-N_1 k ; N_3-N_1

Table III-2

Core levels and contact spin density for each atoms in the clusters.

	FE_9		FE_{15}		
Site	1	2	1	2	3
1s	507.80 507.80	507.83 507.83	507.89 507.89	507.85 507.85	507.84 507.84
2s	58.71 58.73	58.79 58.68	58.81 58.81	58.82 58.71	58.81 58.69
2p	50.68 50.70	50.75 50.66	50.78 50.80	50.77 50.69	50.76 50.67
3s	6.35 6.40	6.53 6.29	6.45 6.46	6.53 6.32	6.53 6.30
3p	4.02 4.07	4.19 3.96	4.12 4.13	4.20 3.99	4.19 3.96
Contact spin density (a.u.)	-0.71	+0.24	-0.08	-0.24	-0.40
E_F	-0.240		-0.299		

Note 1. Site 1, 2, and 3 denote the central, first- and second-shell atoms.

2. Energies are in Ryd. unit and upper (lower) numbers are for majority (minority) spins.

Table C-1

Labelling the Polynomial Type Basis Forms

Note: 1. Vertical number 1, 2, 3, 4, ... denotes J
2. horizontal columns 1, 2, 3 denotes K
3. ℓx denotes angular index assigned.

in the expression CCOE (ℓx, J, K)
LLIJ (ℓx, K, I)

*ℓx = 2

1. $x^2 - y^2 + 0$
2. $0 + y^2 - z^2$
3. $-x^2 + 0 + z^2$

*ℓx = 3

1. $2x^2 - y^2 - z^2$
2. $-x^2 + 2y^2 - z^2$
3. $x^2 - y^2 + 2z^2$

*ℓx = 4

1. x - y + 0
2. x + y + 0
3. 0 + y - z
4. 0 + y + z
5. -x + 0 + z
6. x + 0 + z
7. -
8. -

*ℓx = 5

1. x + y + z
2. x + y - z
3. x - y + z
4. x - y - z
5. x + y + 2z
6. x - y + 2z
7. -x + y + 2z
8. -x - y + 2z

*ℓx = 6

1. xy - yz + 0
2. xy + yz + 0
3. 0 + yz - zx
4. 0 + yz + zx
5. -xy + 0 + zx
6. xy + 0 + zx
7. -
8. -

*ℓx = 7

1. xy + yz + zx
2. xy + yz - zx
3. xy - yz + zx
4. xy - yz - zx
5. 2xy + yz + zx
6. 2xy + yx - zx
7. 2xy - yz + zx
8. 2xy - yz - zx

FIGURE CAPTIONS

Figure III-1. Geometries for the SC-, BCC-, and FCC-systems with up to the second nearest neighbors.

Figure III-2. Energy level diagram for the Fe_9 cluster. The symmetries of levels and the occupancies (N_e) are given. The dashed line shows the position of the Fermi lend at $t_{1u\uparrow}$, and the crosses indicate that it is occupied by two electrons.

Figure III-3. Energy level diagram for the Fe_{15} cluster.

Figure III-4. Integrated density of states for Fe_{15} with majority and minority spins separated. The ordinate shows the number of states per atom Results from the band calculation of Ref. 15 are presented, with the energies shifted so that the Fermi energies of cluster and bulk coincide.

Figure III-5. Integrated density of states for Fe_{15} with spins combined.

Figure III-6. Cluster density of states for Fe_9.

Figure III-7. Cluster density of states for Fe_{15} with majority and minority spins separated. Solid line: present calculation, dashed line, bulk iron from Ref. 15.

Figure III-8. Cluster density of states for fe_{15} with spoin states combined.

Figure III-9. $Fe_{14}C$ total and majority and minority spin density of states.

Figure A-1 Figures arising from the partition of cubes by wedge boundaries.

Figure A-2 Two dimensional cross section of the doubling grid for a one shell BCC system. The cross hatched areas are regions of smaller divisions than those explicitly illustrated.

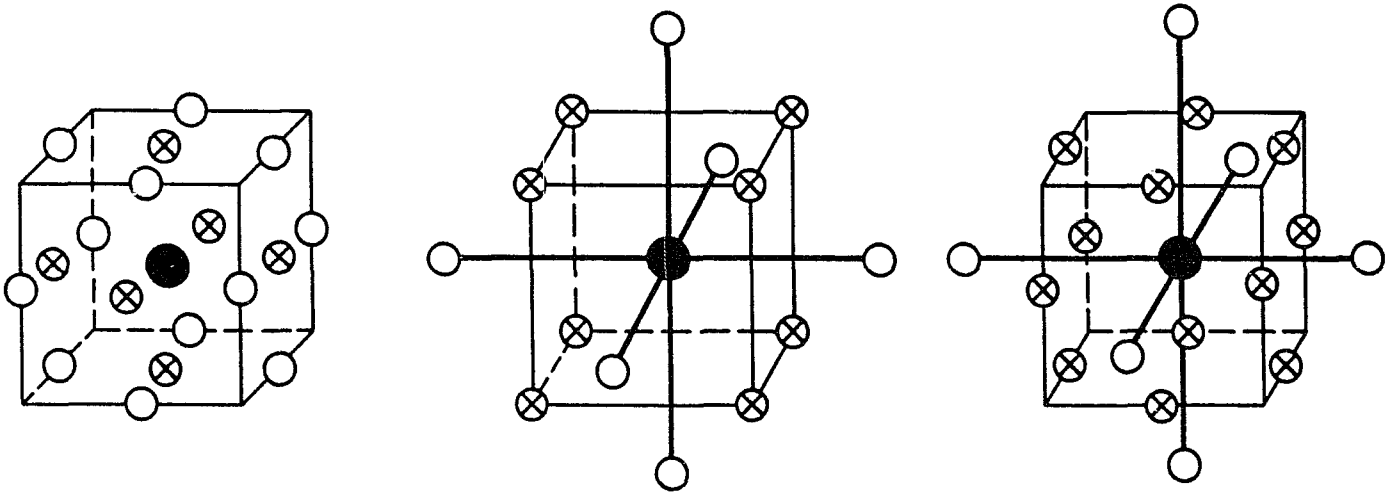

Figure III-1

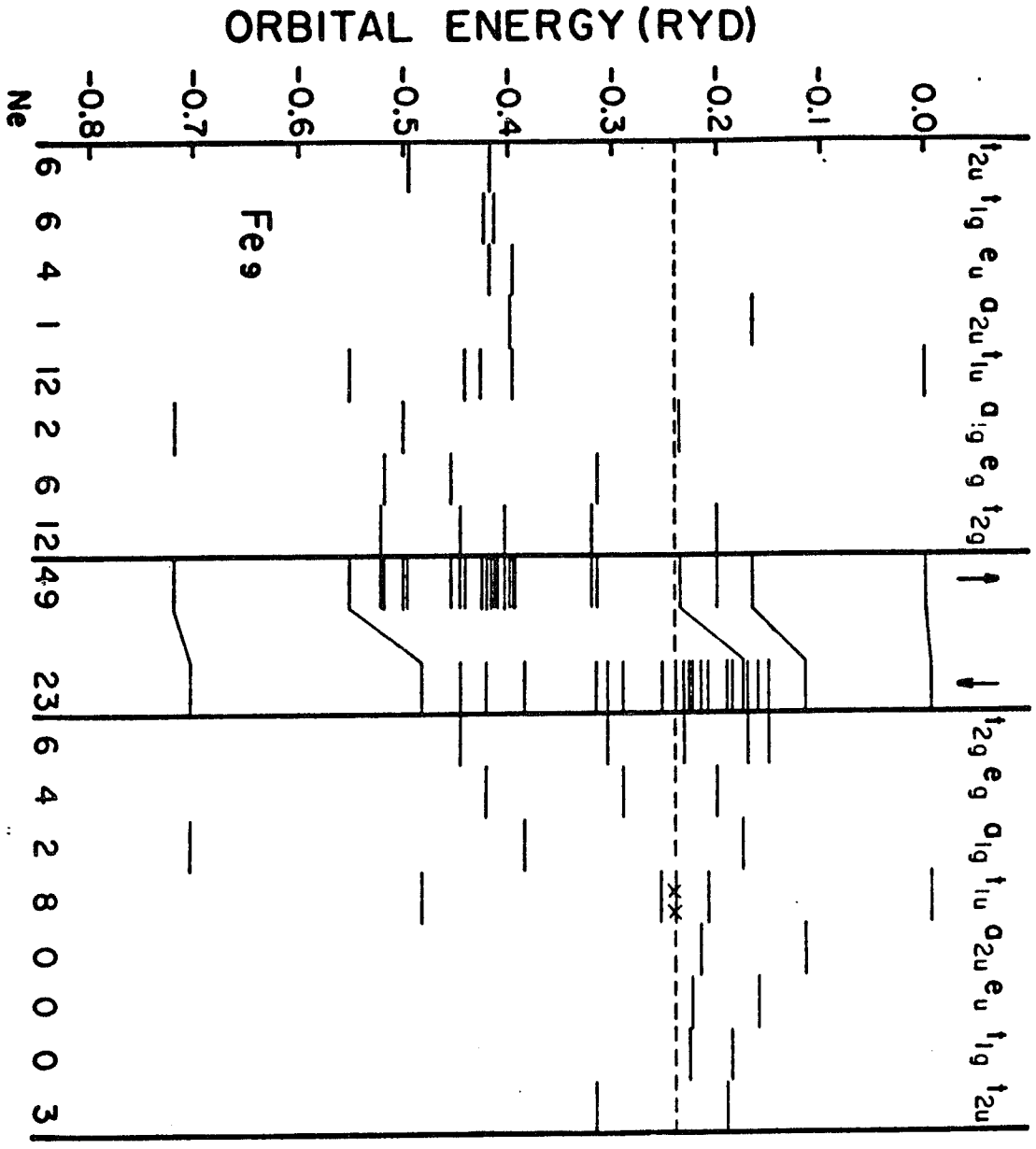
ORBITAL ENERGY (RYD)
-0.8
-0.7
-0.6
-0.5
-0.4
-0.3
-0.2
-0.1
0.0
Ne
6 6 4 1 12 2 6 12 49 23 6 4 2 8 0 0 0 3
Fe 9
t_{2u} t_{1g} e_u a_{2u} t_{1u} a_{1g} e_g t_{2g}
t_{2g} e_g a_{1g} t_{1u} a_{2u} e_u t_{1g} t_{2u}

Figure III-2

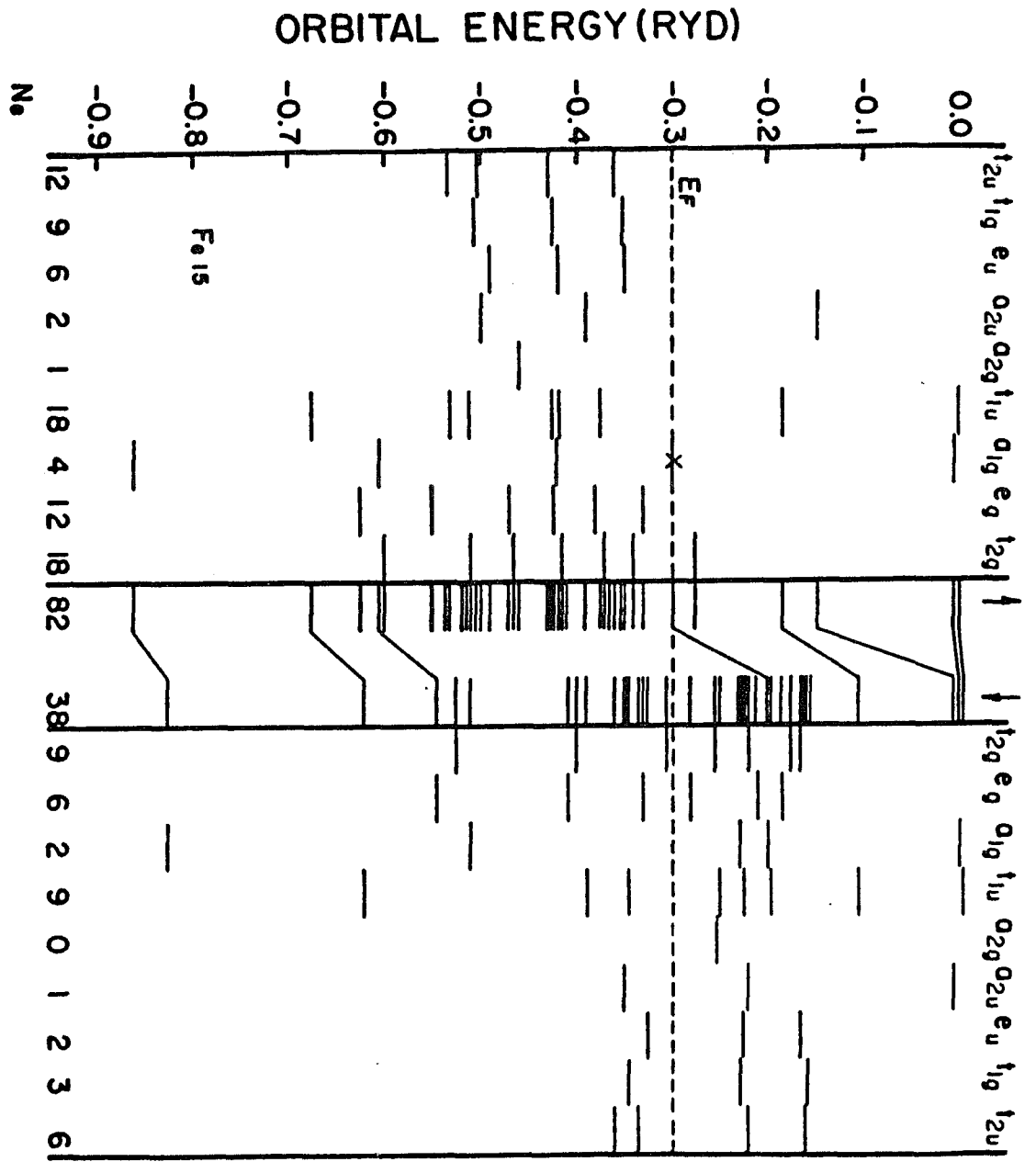
ORBITAL ENERGY (RYD)
No.
-0.9
-0.8
-0.7
-0.6
-0.5
-0.4
-0.3
-0.2
-0.1
0.0
EF
Fe15
12 9 6 2 1 18 4 12 18 82 38 9 6 2 9 0 1 2 3 6
t2u t1g eu a2u a2g t1u a1g eg t2g
t2g eg a1g t1u a2g a2u eu t1g t2u

Figure III-3

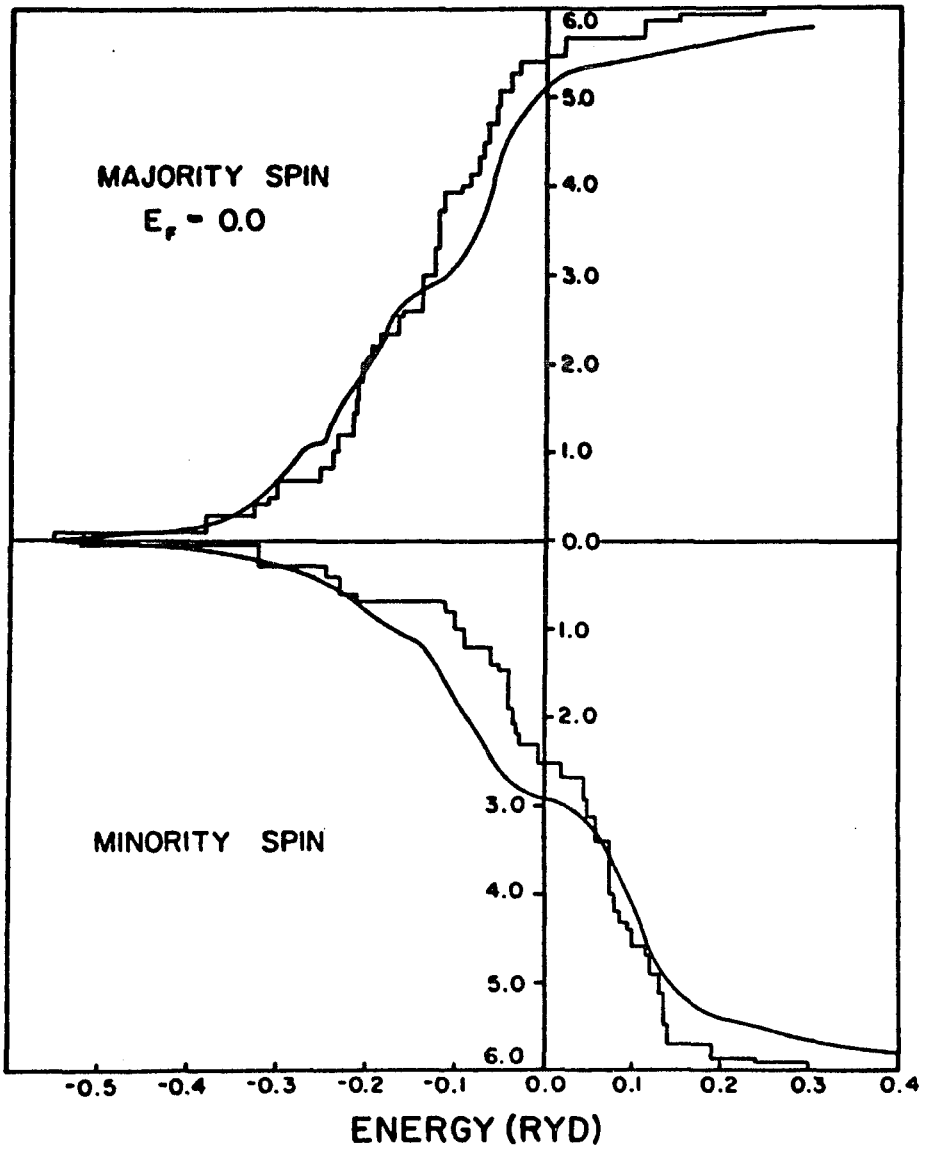
MAJORITY SPIN
E_F = 0.0
MINORITY SPIN
6.0
5.0
4.0
3.0
2.0
1.0
0.0
1.0
2.0
3.0
4.0
5.0
6.0
-0.5
-0.4
-0.3
-0.2
-0.1
0.0
0.1
0.2
0.3
0.4
ENERGY (RYD)

Figure III-4

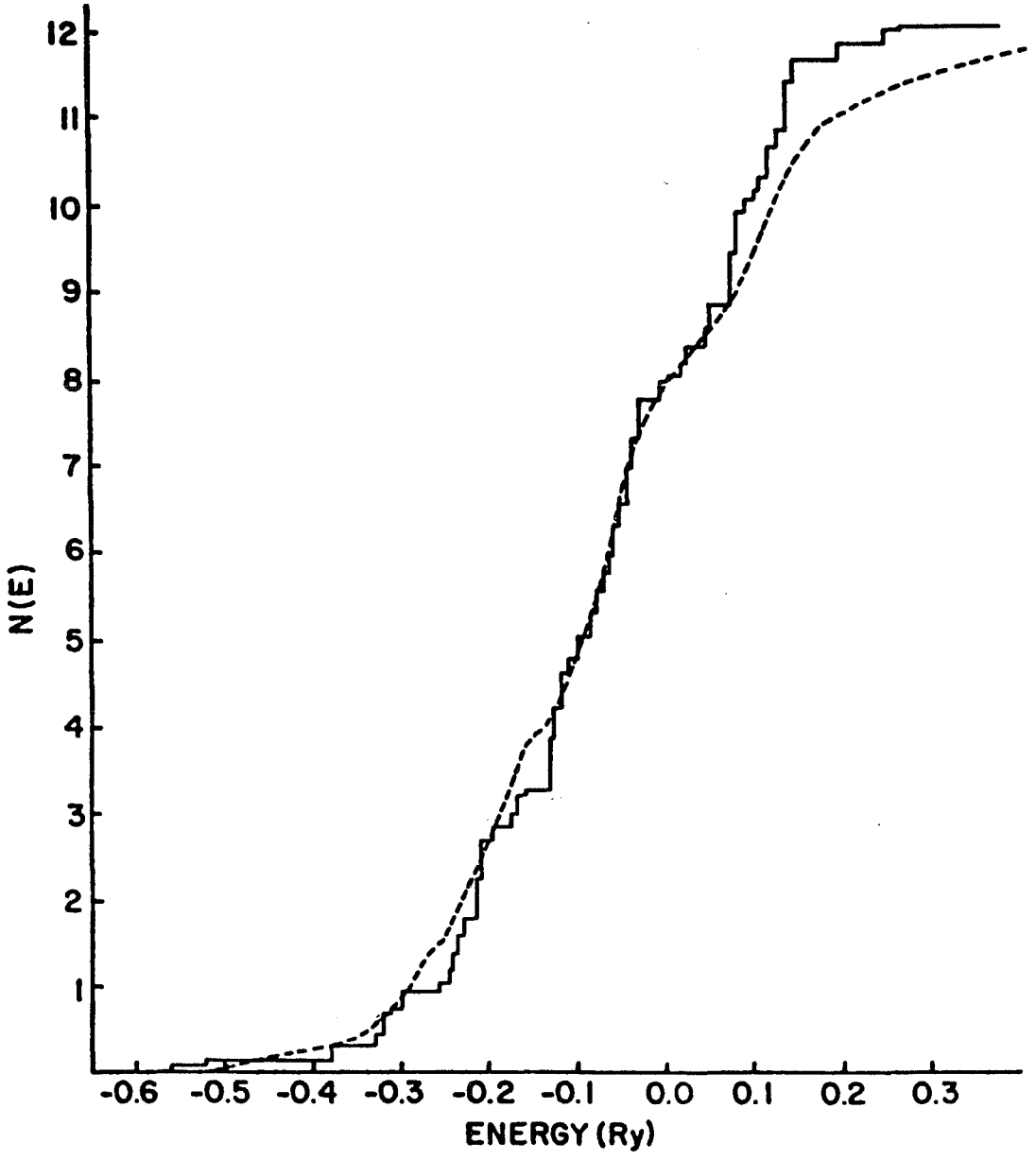

Figure VII-5

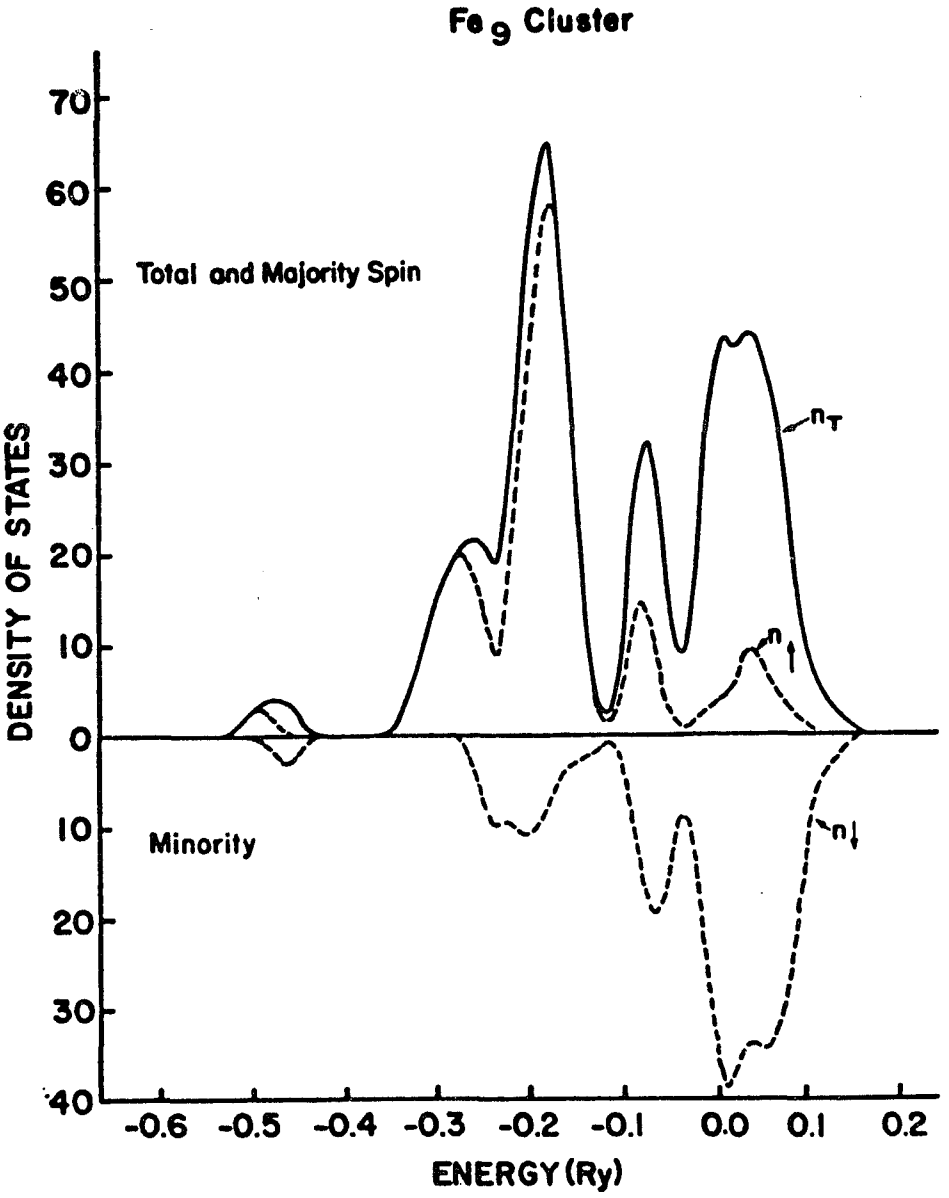
Fe 9 Cluster
Total and Majority Spin
Minority
DENSITY OF STATES
ENERGY (Ry)
70
60
50
40
30
20
10
0
10
20
30
40
-0.6
-0.5
-0.4
-0.3
-0.2
-0.1
0.0
0.1
0.2
n_T
$n_\uparrow$
$n_\downarrow$

Figure III-6

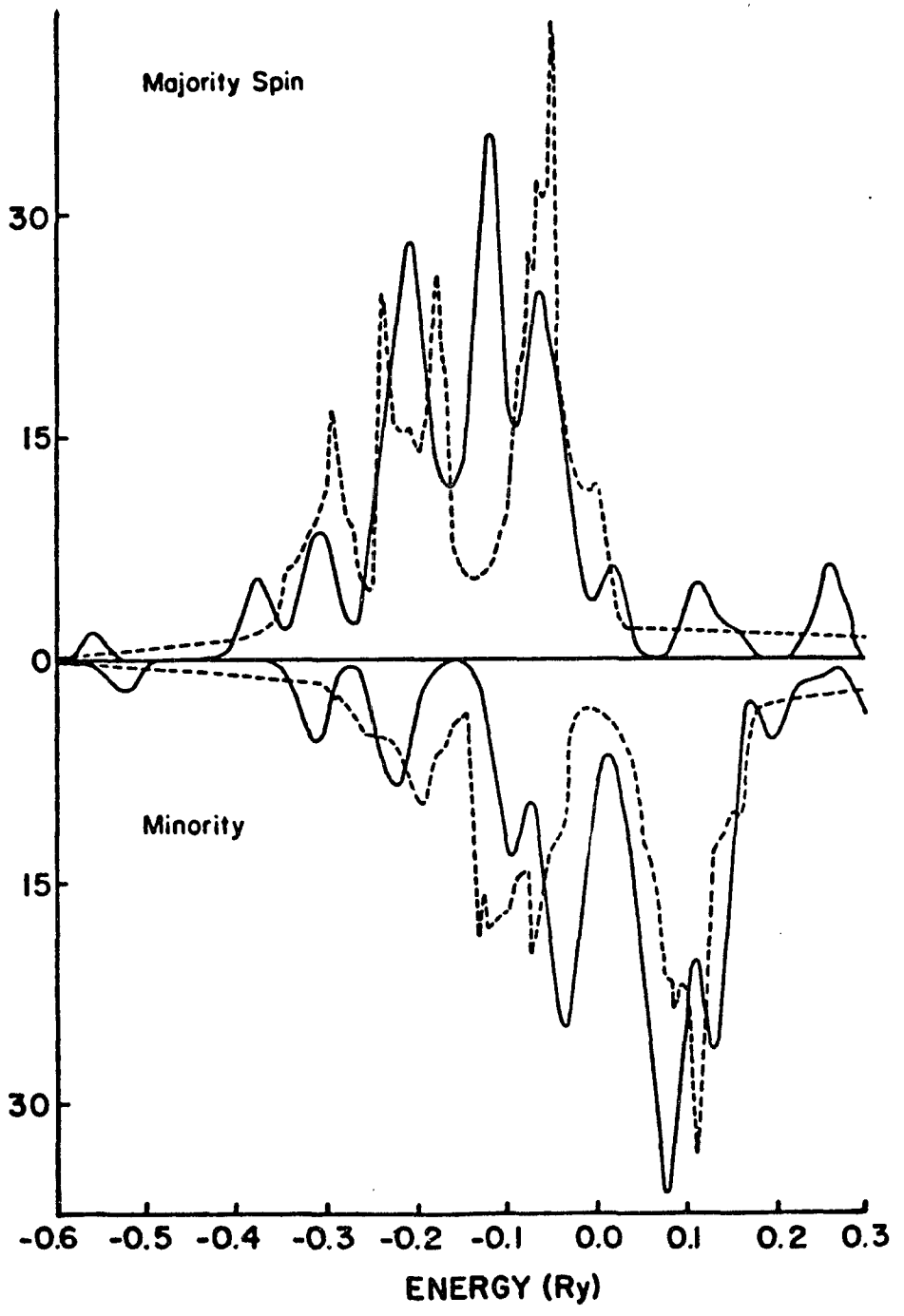
Majority Spin
30
15
0
Minority
15
30
-0.6
-0.5
-0.4
-0.3
-0.2
-0.1
0.0
0.1
0.2
0.3
ENERGY (Ry)

Figure III-7

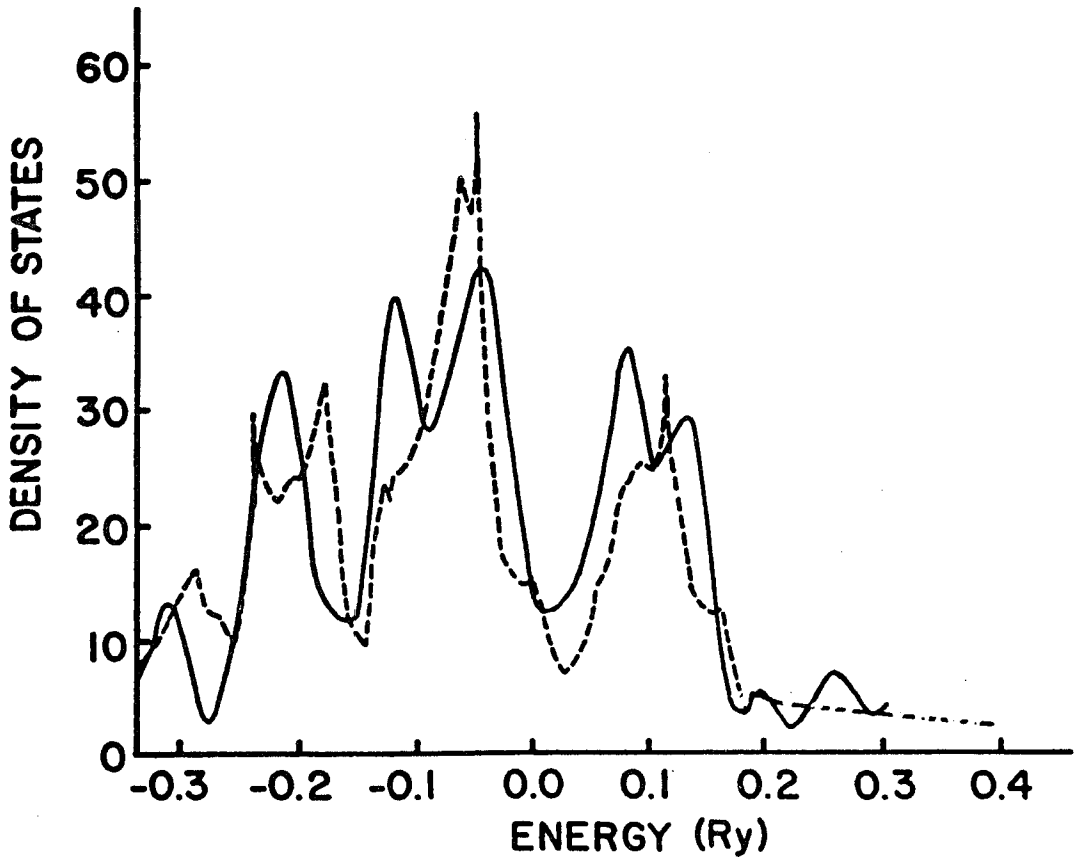
DENSITY OF STATES
60
50
40
30
20
10
0
-0.3
-0.2
-0.1
0.0
0.1
0.2
0.3
0.4
ENERGY (Ry)

Figure III-8

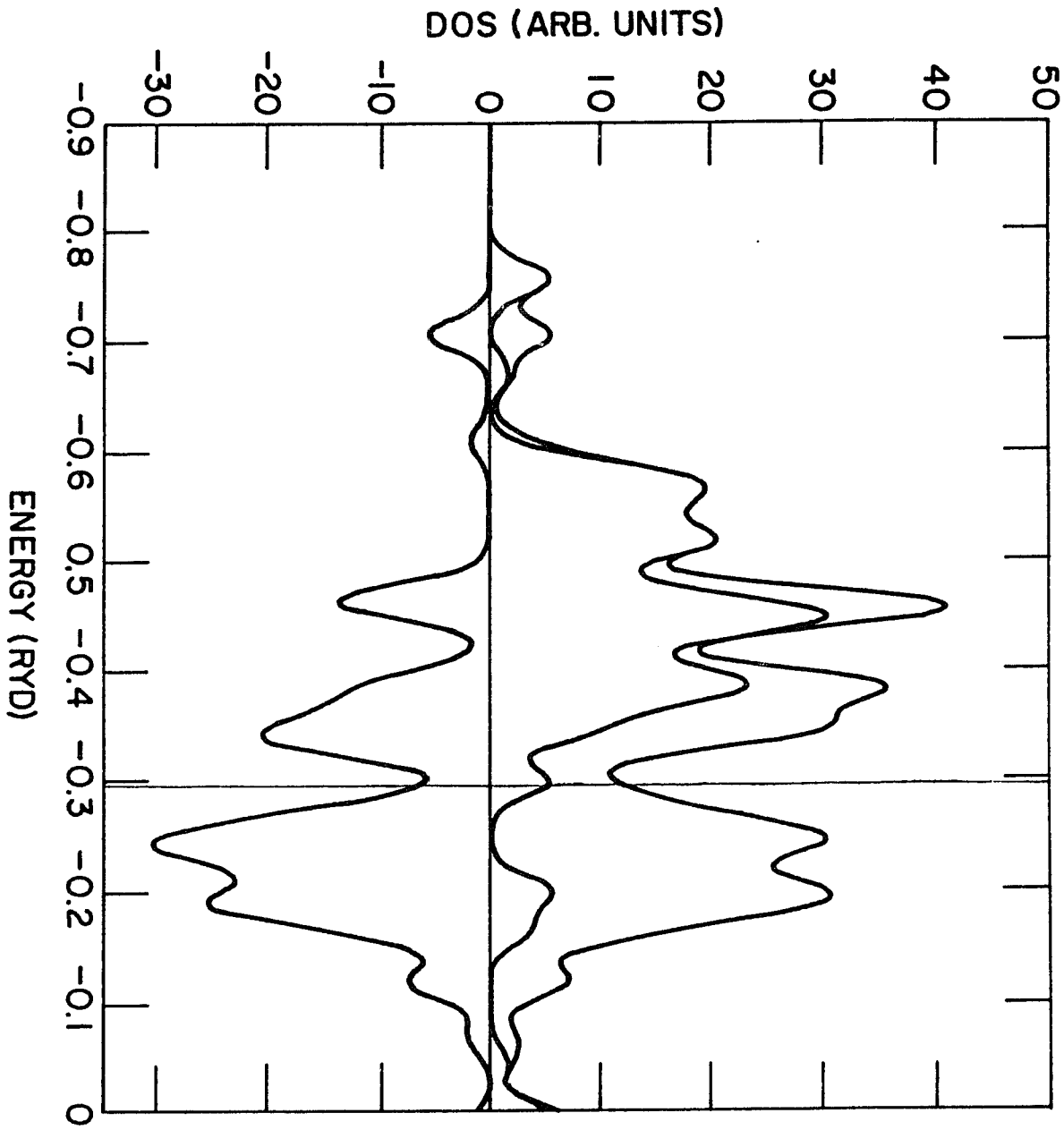
DOS (ARB. UNITS)
-30
-20
-10
0
10
20
30
40
50
ENERGY (RYD)
-0.9
-0.8
-0.7
-0.6
0.5
-0.4
-0.3
-0.2
-0.1
0

Figure III-9

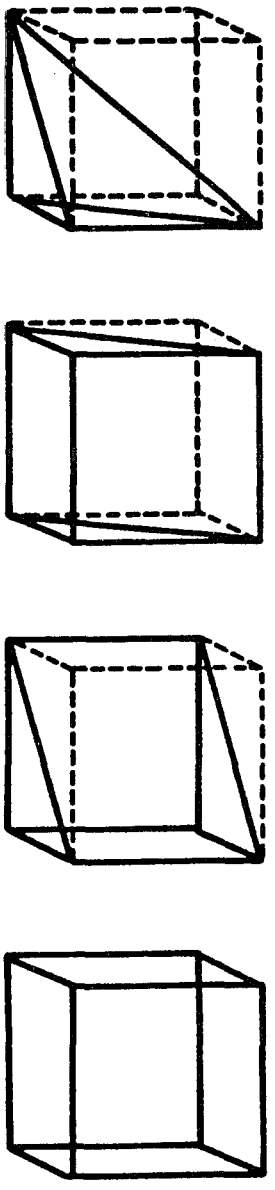

Figure A-1

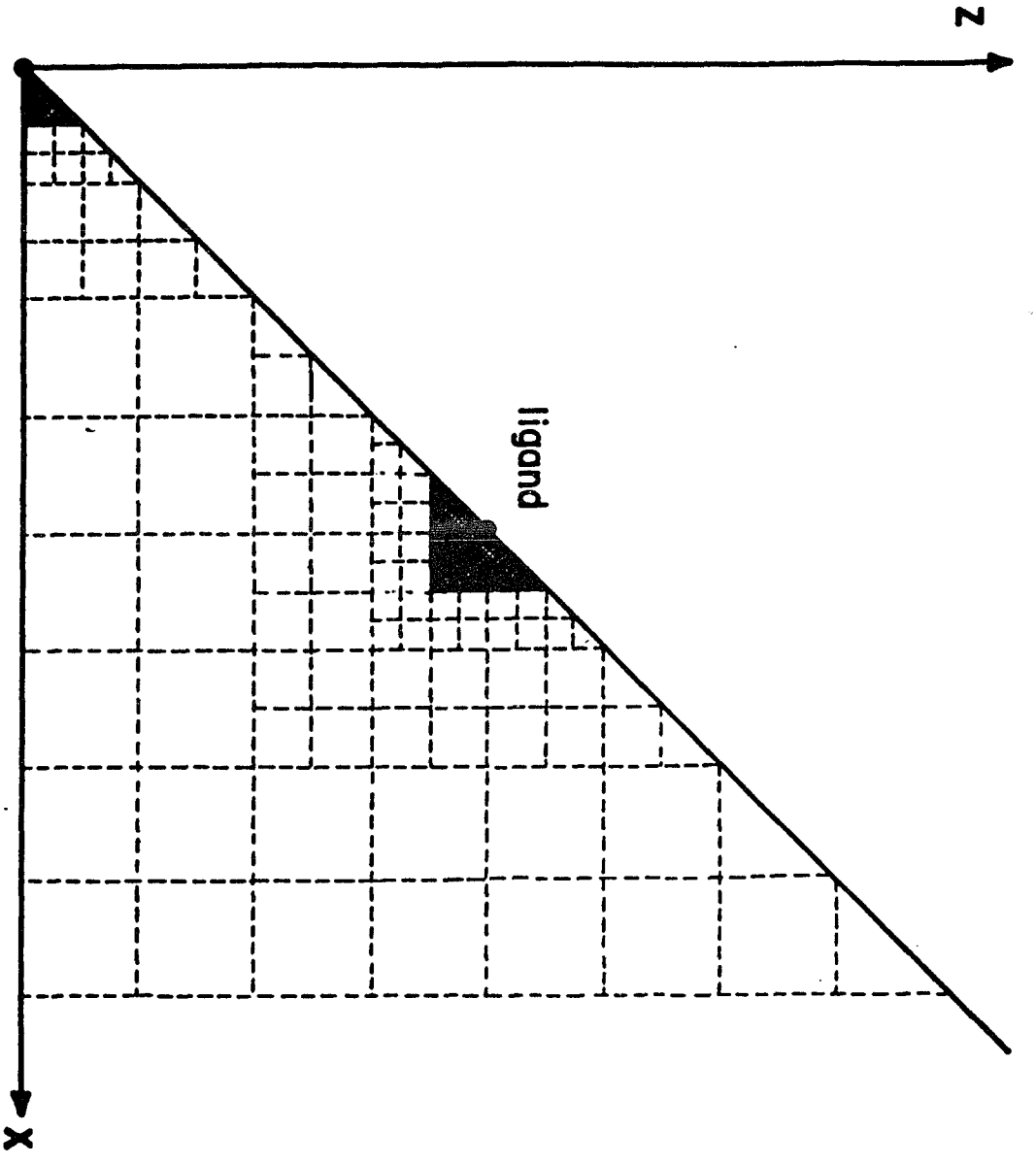

Figure A-2

Appendix A

The Doubling Grid

In our doubling grid, which is intended for cubic geometries, we divide space within the 1/48-th irreducible wedge in several division. Space within each division is filled with elementary cubes of the same size. The size of the elementary cubes are made sufficiently small near atomic centers where some orbital basis functions vary rapidly. The elementary cube size is increased as distances from atomic centers are increased. We could double the elementary cube length for most of the successive divisions except at one stage where "approximate doubling" was used to avoid unnecessary explosion in the number of elementary cubes due to the necessity of rapidly increasing number of sub-divisions.

The sampling points for integration are chosen to be at the center of each elementary cubes even in cases where only part of cube remains within the wedge. This choice of sampling point is obviously natural for cubes which are completely within the wedge and is also natural for cubes having only portions of their volume within the wedge although it can be seen with simple reasoning that we are wasting sampling points by such a choice. Avoiding high symmetry planes may be desirable in placing sampling points but we could not find any other choice of sampling points which could give a better result. For example, we tried shfiting our points to center of mass positions for fractional cubes (in the full cube it remains at the same position) only to get worse results.

Another point of importance is the necessity of choosing comparable cube size for comparable regions of space. If one part of the space were given finer grid due to some interest in the particular region, the integration result became worse for those cases where proper cancellation could not be obtained due to failure to employ a finer grid in other relevant regions.

The fact that we have a situation where we cannot fill the region with cubes only if we go on with strict doubling can be seen with simple reasoning. Consider a two dimensional grid: In the two sub-division case, wehre each doubled length division is divided into two alogn the abscissa within its own division, we have found it acceptable to have basic length increasing by

$$a, 2a, 3a, 6a, 12a, 24a, \ldots.$$

for divisions I, II, III, ... respectively. If this procedure is not followed awkwardly shaped fractionally filled regions result.

The accuracy obtainable from a given grid was evaluated by using the grid to compute overlap integrals. Analytic results for these are easy to obtain for comparison purposes. Since the exchange-correlation potential for which the grid is intended is slowly varying, the overlap integral test should be representative.

In the iron cluster system, we chose II basic doubling for a two sub-division case with a minimum cube length of a=0.00044 a.u., giving a total number of $\approx$ 1300 points in the Fe_9 system and $\approx$ 2100 points in the

Fe_{15} system. The errors in the overlap test are about 3%. Choosing a four sub-division case gave better accuracy with 8 doublings and a minimum cube length of a=0.0015 a.u. This generating ≈ 6300 points in Fe_9 system and yielded about 1% accuracy additional. Four additional doubling regions were added to the above mentioned number of basic doubling regions to extend the integration region into the exterior of the cluster. The errors in our overlap test were almost always underestimates of the magnitude of the integrals. This implies that we may underestimate slightly the magnitude of exchange correlation effects in our calculation.

In the actual implementation of grid generation we filled the space within each division by several typical blocks. Sub-programs were made for each typical block in which all grid points as well as weight factors are generated once the choice of sub-division number along the abscissa and the data for block dimension lengths elementary cube length are provided.

We have found that any elementary region within the wedge takes one of the four shapes shown in Fig. A-1. There is no ambiguity in choosing the sampling points for these shapes which obviously are at the center of the cubes, though this will be on a high symmetry plane in some cases. This in effect, reduces the number of independent sampling points as a result.

A two dimensional cross section of a two sub-division case is sketched in Fig. A-2 (this could be either the BCc or FCC first neighbor situation.

1. APPENDIX B.
2.
3. THE FOLLOWING FUNCTIONAL FORMS WERE CONSTRUCTED USING THE
4. PROJECTION TECHNIQUE OF GENERATING SYMMETRIZED WAVE FUNCTION
5. BASIS WHICH IS DESCRIBED IN DETAIL ELSWHERE(REF.50 AND 51).
6.
7. BASIS FUNCTIONS FOR THE CENTRAL SITE(LOCATED AT THE ORIGIN)
8. ANGULAR FUNCTIONS ARE GIVEN AS FOLLOWS;
9.
10. 1.A1G
11. S=S
12. 2.T1U
13. P=X
14. P=Y
15. P=Z
16. 3.EG
17. D=X*X-Y*Y
18. D=-(2*Z*Z-X*X-Y*Y)
19. 4.T2G
20. D=XY
21. D=YZ
22. D=ZX
23.
24. LEGEND;
25. XXYY=X*X-Y*Y
26. YYZZ=Y*Y-Z*Z
27. ZZXX=Z*Z-X*X
28. XX=2*X*X-Y*Y-Z*Z
29. YY=2*Y*Y-Z*Z-X*X
30. ZZ=2*Z*Z-X*X-Y*Y
31.
32. NOTE 1; NUMBERS WITHIN THE PARENTHESIS FOR EACH IRREDUCIBLE
33. REPRESENTATION SYMBOL INDICATES THE ORDER(DEGENERACY).
34. NOTE 2; FOR BREVITY, ONLY THE SIGNS ARE GIVEN FOR FOLLOWING TERMS
35. WHICH HAVE IDENTICAL ANGULAR TERMS AS THE FIRST TERM.
36. NOTE 3; BLANK PARENTHESIS (0) MEANS NO FUNCTIONS PRESENT.
37.
38.
39. BASIS FOR THE SIMPLE CUBIC SYSTEM
40.
41.
42. POSITIONS ARE ASSIGNED AS
43. 1=(A,0,0)
44. 2=(-A,0,0)
45. 3=(0,A,0)
46. 4=(0,-A,0)
47. 5=(0,0,A)
48. 6=(0,0,-A)
49.
50. AND COMBINATIONS ARE LISTED IN THE ORDER OF
51.
52. BASIS=+(1 2)+(3 4)+(5 6)
53.
54. 1.A1G(1)
55.
56. S=+(+S+S)+(+S+S)+(+S+S)
57. P=+(+X-X)+(+Y-Y)+(+Z-Z)
58. D=+(+XX-XX)+(+YY-YY)+(+ZZ-ZZ)
59.

```
     2.T1U(3)

       S=+(+S-S)+( 0 )+( 0 )
       S=+( 0 )+(+S-S)+( 0 )
       S=+( 0 )+( 0 )+(+S-S)

       P=+(+X+X)+( 0 )+( 0 )
       P=+( 0 )+(+Y+Y)+( 0 )
       P=+( 0 )+( 0 )+(+Z+Z)

       P=+( 0 )+(+X+X)+(+X+X)
       P=+(+Y+Y)+( 0 )+(+Y+Y)
       P=+(+Z+Z)+(+Z+Z)+( 0 )

       D=+( 0 ) +(+XY-XY)+(+ZX-ZX)
       D=+(+XY-XY)+( 0 )+(+YZ-YZ)
       D=+(+ZX-ZX)+(+YZ-YZ)+( 0 )

       D=+(+XX-XX)+( 0 )+( 0 )
       D=+( 0 )+(+YY-YY)+( 0 )
       D=+( 0 )+( 0 )+(+ZZ-ZZ)

     3.T1G(3)

       P=+( 0 )+(-Z+Z)+(+Y-Y)
       P=+(+Z-Z)+( 0 )+(-X+X)
       P=+(-Y+Y)+(+X-X)+( 0 )

       D=+( 0 )+(+YZ+YZ)+(-YZ-YZ)
       D=+(-ZX-ZX)+( 0 )+(+ZX+ZX)
       D=+(+XY+XY)+(-XY-XY)+( 0 )

     4.T2U(3)

       P=+(+Z+Z)+(-Z-Z)+( 0 )
       P=+( 0 )+(+X+X)+(-X-X)
       P=+(-Y-Y)+( 0 )+(+Y+Y)

       D=+(+ZX-ZX)+(-YZ+YZ)+( 0 )
       D=+( 0 )+(+XY-XY)+(-ZX+ZX)
       D=+(-XY+XY)+( 0 )+(+YZ-YZ)

       D=+( 0 )+( 0 )+(+XXYY-XXYY)
       D=+(+YYZZ-YYZZ)+( 0 )+( 0 )
       D=+( 0 )+(+ZZXX-ZZXX)+( 0 )

     5.T2G(3)

       P=+(+Y-Y)+(+X-X)+( 0 )
       P=+( 0 )+(+Z-Z)+(+Y-Y)
       P=+(+Z-Z)+( 0 )+(+X-X)

       D=+( 0 )+( 0 )+(+XY+XY)
       D=+(+YZ+YZ)+( 0 )+( 0 )
       D=+( 0 )+(+ZX+ZX)+( 0 )

       D=+(+XY+XY)+(+XY+XY)+( 0 )
       D=+( 0 )+(+YZ+YZ)+(+YZ+YZ)
       D=+(+ZX+ZX)+( 0 )+(+ZX+ZX)
```

```
120.     6.EG(2)
121.
122.       S=+(+S+S)+(-S-S)+( 0 )
123.       S=+(+S+S)+(+S+S)+(-2)(+S+S)
124.
125.       P=+(+X-X)+(-Y+Y)+( 0 )
126.       P=+(+X-X)+(+Y-Y)+(-2)(+Z-Z)
127.
128.       D=+(+XX+XX)+(-YY-YY)+( 0 )
129.       D=+(+XX+XX)+(+YY+YY)+(-2)(+ZZ+ZZ)
130.
131.       D=+(+YYZZ+YYZZ)+(+ZZXX+ZZXX)+(-2)(+XXYY-XXYY)
132.       D=+(-YYZZ-YYZZ)+(+ZZXX+ZZXX)
133.
134.     7.EU(2)
135.
136.       D=+(+YZ-YZ)+(-ZX+ZX)+( 0 )
137.       D=+(+YZ-YZ)+(+ZX-ZX)+(-2)(+XY-XY)
138.
139.     8.A2U(1)
140.
141.       D=+(+YYZZ+YYZZ)+(+ZZXX+ZZXX)+(+XXYY+XXYY)
142.
143.     9.A2G(1)
144.
145.       D=+(+YZ-YZ)+(+ZX-ZX)+(+XY-XY)
146.
147.         ================
148.
```

APPENDIX C.

BASIS FOR THE BODY-CENTERED CUBIC SYSTEM

POSITIONS ARE ASSIGNED AS
1=(A, A, A)
2=(A, A,-A)
3=(A,-A, A)
4=(A,-A,-A)
5=(-A, A, A)
6=(-A, A,-A)
7=(-A,-A, A)
8=(-A,-A,-A)

COMBINATIONS ARE LISTED IN THE ORDER OF
BASIS=(1 2 3 4)+(5 6 7 8)

1.A1G(1)

S=+(+S+++)+(+S+++)
P=+(+X+Y+Z)+(++-)+(+-+)+(+--)
-(+--) -(+-+)-(++-)-(+++)
D=+(+XY+YZ+ZX)+(+--)-(++-)-(+-+)
-(+-+) -(++-)+(+--)+(+++)

2.A2U(1)

S=+(+S--+)+(-S++-)
P=+(+X+Y+Z)-(++-)-(+-+)+(+--)
+(+--)-(+-+)-(++-)+(+++)
D=+(+XY+YZ+ZX)-(+--)+(++-)-(+-+)
+(+-+) -(++-)+(+--)-(+++)

3.T1G(3)

S=+(+S+++)+(-S---)
S=+(+S+--)+(+S+--)
S=+(+S-+-)+(+S-+-)

P=+(+X+++)+(+X+++)
P=+(+Y+++)+(+Y+++)
P=+(+Z+++)+(+Z+++)

P=+(+Y+Z)+(+-)-(+-)-(++)
-(++) -(+-)+(+-)+(++)
P=+(+Z+X)-(+-)-(++)+(+-)
+(+-) -(++)-(+-)+(++)
P=+(+X+Y)-(++)+(+-)-(+-)
-(+-)+(+-)-(++)+(++)

D=+(+YZ--+)+(-YZ++-)
D=+(+ZX--+)+(-ZX++-)
D=+(+XY--+)+(-XY++-)

D=+(+ZX+XY)-(+-)+(+-)-(++)
+(++) -(+-)+(+-)-(++)
D=+(+XY+YZ)+(+-)+(++)+(+-)
-(+-) -(++)-(+-)-(++)
D=+(+YZ+ZX)+(++)-(+-)-(+-)

```
      +(+-)  +(+-)-(++)-(++)

  D=+(+XX+++)+(-XX---)
  D=+(+YY+--)+(+YY+--)
  D=+(+ZZ-+-)+(+ZZ-+-)
```

4.T1U(3)

```
  P=+(+Y-Z)-(++)+(++)-(+-)
    +(+-)  -(++)+(++)-(+-)
  P=+(+Z-X)+(++)+(+-)+(++)
    -(++)  -(+-)-(++)-(+-)
  P=+(+X-Y)+(+-)-(++)-(++)
    +(++)  +(++)-(+-)-(+-)

  D=+(+ZX-XY)+(++)-(++)-(+-)
    -(+-)    -(++)+(++)+(+-)
  D=+(+XY-YZ)-(++)-(+-)+(++)
    +(++)    -(+-)-(++)+(+-)
  D=+(+YZ-ZX)-(+-)+(++)-(++)
    -(++)    +(++)-(+-)+(+-)

  D=+(+YYZZ--+)+(+YYZZ--+)
  D=+(+ZZXX+--)+(-ZZXX-++)
  D=+(+XXYY+--)+(-XXYY-++)
```

5.T2U(3)

```
  P=+(+X-Y)-(+-)+(++)-(++)
    -(++)  +(++)-(+-)+(+-)
  P=+(+Y-Z)+(++)-(++)-(+-)
    -(+-)  -(++)+(++)+(+-)
  P=+(+Z-X)-(++)-(+-)+(++)
    +(++)  -(+-)-(++)+(+-)

  D=+(+YZ-ZX)+(+-)-(++)-(++)
    +(++)    +(++)-(+-)-(+-)
  D=+(+ZX-XY)-(++)+(++)-(+-)
    +(+-)    -(++)+(++)-(+-)
  D=+(+XY-YZ)+(++)+(+-)+(++)
    -(++)    -(+-)-(++)-(+-)

  D=+(+XXYY-+-)+(+XXYY-+-)
  D=+(+YYZZ+--)+(+YYZZ+--)
  D=+(+ZZXX+--)+(+ZZXX+--)
```

6.T2G(3)

```
  S=+(+S+--)+(-S-++)
  S=+(+S--+)+(+S--+)
  S=+(+S-+-)+(-S+-+)

  P=+(+Z--+)+(-Z++-)
  P=+(+X--+)+(-X++-)
  P=+(+Y--+)+(-Y++-)

  P=+(+X+Y)+(++)-(+-)-(+-)
    +(+-)  +(+-)-(++)-(++)
  P=+(+Y+Z)-(+-)+(+-)-(++)
    +(++)  -(+-)+(+-)-(++)
```

```
P=+(+Z+X)+(+-)+(++)+(+-)
  -(+-)  -(++)-(+-)-(++)

D=+(+XY+++)+(+XY+++)
D=+(+YZ+++)+(+YZ+++)
D=+(+ZX+++)+(+ZX+++)

D=+(+ZZ+--)+(-ZZ-++)
D=+(+YY-+-)+(-YY+-+)
D=+(+YY-+-)+(-YY+-+)

D=+(+YZ+ZX)-(++)+(+-)-(+-)
  -(+-)   +(+-)-(++)+(++)
D=+(+ZX+XY)+(+-)-(+-)-(++)
  -(++)    -(+-)+(+-)+(++)
D=+(+XY+YZ)-(+-)-(++)+(+-)
  +(+-)    -(++)-(+-)+(++)
```

7.EG(2)

```
P=+(+X-Y)+(+-)+(++)+(++)
  -(++)  -(++)-(+-)-(+-)
P=-(+2Z-X-Y)+(+++)-(+-+)+(++-)
  -(++-)    +(+-+)-(+++)+(++-)

D=+(+YZ-ZX)-(+-)-(++)+(++)
  +(++)    -(++)-(+-)+(+-)
D=-(2XY-YZ-ZX)-(+++)+(+-+)+(++-)
  +(++-)      +(+-+)-(+++)-(+--)

D=+(+XXYY+++)+(+XXYY+++)
D=+(-ZZ---)+(-ZZ---)
```

8.EU(2)

```
P=-(2Z-X-Y)-(+++)+(+-+)+(++-)
  +(++-)   +(+-+)-(+++)-(+--)
P=+(+X-Y)-(+-)-(++)+(++)
  +(++)  -(++)-(+-)+(+-)

D=-(2XY-YZ-ZX)+(+++)-(+-+)+(++-)
  -(++-)      +(+-+)-(+++)+(+--)
D=+(+YZ-ZX)+(+-)+(++)+(++)
  -(++)    -(++)-(+-)-(+-)

D=+(-ZZ++-)+(+ZZ--+)
D=+(+XXYY--+)+(-XXYY++-)
```

APPENDIX D.

BASIS FOR THE FACE-CENTERED CUBIC SYSTEM.

```
POSITIONS ARE ASSIGNED AS
  1=( A, A, 0 )
  2=( A,-A, 0 )
  3=(-A, A, 0 )
  4=(-A,-A, 0 )
  5=( 0, A, A)
  6=( 0, A,-A)
  7=( 0,-A, A)
  8=( 0,-A,-A)
  9=( A  0, A)
 10=(-A, 0, A)
 11=( A, 0,-A)
 12=(-A, 0,-A)

BASIS FUNCTIONS ARE GIVEN IN THE ORDER OF
  BASIS=(1 2 3 4)+(5 6 7 8)+(9 10 11 12)

1.A1G(1)

  S=+(+S+++)+(+S+++)+(+S+++)
  P=+(+(X+Y)+(+-)-(+-)-(++))
    +(+(Y+Z)+(+-)-(+-)-(++))
    +(+(Z+X)+(+-)-(+-)-(++))
  D=+(+XY--+)+(+YZ--+)+(+ZX--+)
  D=+(+ZZ+++)+(+XX+++)+(+YY+++)

2.A1U(1)

  D=+(-(YZ-ZX)-(++)+(++)+(+-))
   +(-(ZX-XY)-(++)+(++)+(+-))
   +(-(XY-YZ)-(++)+(++)+(+-))

3.A2G(1)

  P=+(+(X-Y)+(++)-(++)-(+-))
   +(+(Y-Z)+(++)-(++)-(+-))
   +(+(Z-X)+(++)-(++)-(+-))
  D=+(+XXYY+++)+(+YYZZ+++)+(+ZZXX+++)

4.A2U(1)

  P=+(+Z--+)+(+X--+)+(+Y--+)
  D=+(+(YZ+ZX)+(+-)-(+-)-(++))
   +(+(ZX+XY)+(+-)-(+-)-(++))
   +(+(XY+YZ)+(+-)-(+-)-(++))

5.T1U(3)

  S=+(+S+--)+( 0 )+(+S-+-)
  S=+(+S-+-)+(+S+--)+( 0 )
  S=+( 0 )+(+S-+-)+(+S+--)

  P=+( 0 )+(+X+++)+( 0 )
```

```
P=+( 0 )+( 0 )+(+Y+++)
P=+(+Z+++)+( 0 )+( 0 )

P=+(+X+++)+( 0 )+(+X+++)
P=+(+Y+++)+(+Y+++)+( 0 )
P=+( 0 )+(+Z+++)+(+Z+++)

P=+(+Y--+)+( 0 )+(+Z--+)
P=+(+X--+)+(+Z--+)+( 0 )
P=+( 0 )+(+Y--+)+(+X--+)

D=+(+XY-+-)+( 0 )+(+ZX+--)
D=+(+XY+--)+(+YZ-+-)+( 0 )
D=+( 0 )+(+YZ+--)+(+ZX-+-)

D=+( 0 )+(+(ZX+XY)-(+-)+(+-)-(++))+( 0 )
D=+( 0 )+( 0 )+(+(XY+YZ)-(+-)+(+-)-(++))
D=+(+(YZ+ZX)-(+-)+(+-)-(++))+( 0 )+( 0 )

D=+(+ZZXX+--)+( 0 )+(-XXYY+-+)
D=+(-YYZZ+-+)+(+XXYY+--)+( 0 )
D=+( 0 )+(-ZZXX+-+)+(+YYZZ+--)

D=+(+XXYY+--)+( 0 )+(-ZZXX+-+)
D=+(-XXYY+-+)+(+YYZZ+--)+( 0 )
D=+( 0 )+(-YYZZ+-+)+(+ZZXX+--)
```

6.T1S(3)

```
S=+(-Z+-+)+( 0 )+(+Y+--)
S=+(+Z+--)+(-X+-+)+( 0 )
S=+( 0 )+(+X+--)+(-Y+-+)

P=+( 0 )+(+(Y-Z)-(++)+(++)-(+-))+( 0 )
P=+( 0 )+( 0 )+(+(Z-X)-(++)+(++)-(+-))
P=+(+(X-Y)-(++)+(++)-(+-))+( 0 )+( 0 )

D=+(-YZ---)+( 0 )+(+YZ+++)
D=+(+ZX+++)+(-ZX---)+( 0 )
D=+( 0 )+(+XY+++)+(-XY---)

D=+(+ZX--+)+( 0 )+(-XY++-)
D=+(-YZ++-)+(+XY--+)+( 0 )
D=+( 0 )+(-ZX++-)+(+YZ--+)

D=+( 0 )+(+YYZZ--+)+( 0 )
D=+( 0 )+( 0 )+(+ZZXX--+)
D=+(+XXYY--+)+( 0 )+( 0 )
```

7.T2U(3)

```
S=+( 0 )+(-S+-+)+(+S+--)
S=+(+S+--)+( 0 )+(-S+-+)
S=+(-S+-+)+(+S+--)+( 0 )

P=+( 0 )+(+Z+++)+(-Z---)
P=+(-X---)+( 0 )+(+X+++)
P=+(+Y+++)+(-Y---)+( 0 )

P=+( 0 )+(+Y--+)+(-X++-)
```

```
P=+(-Y++-)+( 0 )+(+Z--+)
P=+(+X--+)+(-Z++-)+( 0 )

D=+(-(YZ-ZX)+(++)-(++)+(+-))+( 0 )+( 0 )
D=+( 0 )+(-(ZX-XY)+(++)-(++)+(+-))+( 0 )
D=+( 0 )+( 0 )+(-(XY-YZ)+(++)-(++)+(+-))

D=+( 0 )+(+YYZZ-+-)+(+ZZXX+--)
D=+(+XXYY+--)+( 0 )+(+ZZXX-+-)
D=+(+XXYY-+-)+(+YYZZ+--)+( 0 )

D=+( 0 )+(+ZZXX-+-)+(+YYZZ+--)
D=+(+ZZXX+--)+( 0 )+(+XXYY-+-)
D=+(+YYZZ-+-)+(+XXYY+--)+( 0 )

D=+( 0 )+(+YZ+--)+(-ZX+-+)
D=+(-XY+-+)+( 0 )+(+ZX+--)
D=+(+XY+--)+(-YZ+-+)+( 0 )
```

8.T2G(3)

```
S=+(+S--+)+( 0 )+( 0 )
S=+( 0 )+(+S--+)+( 0 )
S=+( 0 )+( 0 )+(+S--+)

P=+(+(X+Y)-(+-)+(+-)-(++))+( 0 )+( 0 )
P=+( 0 )+(+(Y+Z)-(+-)+(+-)-(++))+( 0 )
P=+( 0 )+( 0 )+(+(Z+X)-(+-)+(+-)-(++))

P=+( 0 )+(+X+--)+(+Y-+-)
P=+(+Z-+-)+( 0 )+(+Y+--)
P=+(+Z+--)+(+X-+-)+( 0 )

D=+(+XY+++)+( 0 )+( 0 )
D=+( 0 )+(+YZ+++)+( 0 )
D=+( 0 )+( 0 )+(+ZX+++)

D=+( 0 )+(+ZX--+)+(+YZ--+)
D=+(+ZX--+)+( 0 )+(+XY--+)
D=+(+YZ--+)+(+XY--+)+( 0 )

D=+( 0 )+(+XY+++)+(+XY+++)
D=+(+YZ+++)+( 0 )+(+YZ+++)
D=+(+ZX+++)+(+ZX+++)+( 0 )

D=+(-ZZ++-)+( 0 )+( 0 )
D=+( 0 )+(-XX++-)+( 0 )
D=+( 0 )+( 0 )+(-YY++-)
```

9.EG(2)

```
S=+( 0 )+(-S---)+(+S+++)
S=+(+2)(+S+++)+(-S---)+(-S---)

P=+( 0 )+(+(Y+Z)+(+-)-(+-)-(++))+(-(Z+X)-(+-)+(+-)+(++))
P=+(+2)(+(X+Y)+(+-)-(+-)+(++))+(-(Y+Z)-(+-)+(+-)+(++))
                               +(-(Z+X)-(+-)+(+-)+(++))

P=+(-2)(+(X-Y)+(++)-(++)-(++))+(+(Y-Z)+(++)-(++)-(+-))
                               +(+(Z-X)+(++)-(++)-(+-))
```

```
  P=+( 0 )+(+(Y-Z)+(++)-(++)-(+-))+(-(Z-X)-(++)+(++)+(+-))

  D=+( 0 )+(-YZ++-)+(+ZX--+)
  D=+(+2)(+XY--+)+(-YZ++-)+(-ZX++-)

  D=+( 0 )+(+XX+++)+(-YY---)
  D=+(-2)(+ZZ+++)+(+XX+++)+(+YY+++)

  D=+(+2)(+XXYY+++)+(-YYZZ---)+(-ZZXX---)
  D=+( 0 )+(+YYZZ+++)+(-ZZXX---)

10.EU(2)

  P=+(+2)(-Z++-)+(+X--+)+(+Y--+)
  P=+( 0 )+(+X--+)+(-Y++-)

  D=+( 0 )+(+(ZX-XY)+(++)-(++)-(+-))+(-(XY-YZ)-(++)+(++)+(+-))
  D=+(+2)(+(YZ-ZX)+(++)-(+-)-(+-))+(-(ZX-XY)-(++)+(++)+(+-))
                                   +(-(XY-YZ)-(++)+(++)+(+-))

  D=+(+2)(+(YZ+ZX)+(+-)-(+-)-(++))+(-(ZX+XY)-(+-)+(+-)+(++))
                                   +(-(XY-YZ)-(+-)+(+-)+(++))
  D=+( 0 )+(-(ZX+XY)-(+-)+(+-)+(++))+(+(XY+YZ)+(+-)-(+-)-(++))
```

VITA

The author was born July 22, 1949, in Inchon, Korea and has received his B.S. degree in Physics from Seoul National University in Seoul, Korea in 1972. He attended Sogang University graduate school in Seoul, Korea and was graduated with a M.S. degree in Physics in 1975. He has taught briefly in a high school in Korea and entered LSU graduate school in 1977. He worked briefly under Professor J. Kimball and A. K. Rajagopal on spin glass problems and continued to work on molecular orbital calculation of large transition metal clusters under Professor J. Callaway afterwards. He is currently employed at Argonne National Laboratory as a Research Associate.

EXAMINATION AND THESIS REPORT

Candidate: Keeyung Lee

Major Field: Physics and Astronomy

Title of Thesis: Electronic Structure of Small Iron Clusters

Approved:

Joseph Callaway
Major Professor and Chairman

Dean of the Graduate School

EXAMINING COMMITTEE:

R C Goodrich

A Marshak

AK Rajagopal

Chin H. Keene

Date of Examination:

March 12, 1984